AN APPROXIMATE RIEMANN SOLVER FOR COMPRESSIBLE FLOWS WITH AXIAL SYMMETRY

P. GLAISTER

NUMERICAL ANALYSIS REPORT 2/87

DEPARTMENT OF MATHEMATICS
P.O. BOX 220
UNIVERSITY OF READING
WHITEKNIGHTS
READING
BERKSHIRE
RG6 2AX

This work forms part of the research programme of the Institute for Computational Fluid Dynamics at the Universities of Oxford and Reading and was funded by A.W.R.E., Aldermaston under contract no. NSN/13B/2A88719.

ABSTRACT

An approximate (linearised) Riemann solver is presented for the solution of the Euler equations of gas dynamics in an orthogonal curvilinear coordinate system. The scheme incorporates the technique of operator splitting. The specific case of axially symmetric flow is discussed in detail and numerical results are given for two test problems.

1. INTRODUCTION

The (linearised) approximate Riemann solver of Roe [1] and extensions given by Glaister [2] have been highly successful in applications to problems governed by the Euler equations with slab, cylindrical or spherical symmetry. We seek here to extend these techniques to multi-dimensional problems, incorporating the technique of operator splitting, including problems with axial symmetry and/or source terms. The resulting method is applied to some strongly shocked axially symmetric flows.

In §2 we review in detail differential equations for the flow of an inviscid perfect gas in a general orthogonal curvilinear coordinate system for the general equations of fluid flow. This is done in order to make clear the origin of the non-cartesian terms in the subsequent equations. In §3 we describe the details of the flux difference splitting scheme for the approximate solution of the equations given in §2, and in §4 we discuss the particular case of axially symmetric flow. Finally in §5 we describe two test problems with axial symmetry and display the numerical results achieved for these two problems using the scheme of §4.

2. EQUATIONS OF FLOW

In this section we consider the Euler equations for modelling the time-dependent flow of an inviscid compressible fluid in a general orthogonal curvilinear co-ordinate system (x_1,x_2,x_3).

The Euler equations governing the flow of a compressible inviscid fluid can be written as

$$\rho_t + \mathrm{div}(\rho\underline{u}) = 0 \tag{2.1}$$

$$(\rho\underline{u})_t + \mathrm{div}(\rho\underline{u}\underline{u}) = -\,\mathrm{grad}\,p \tag{2.2}$$

$$e_t + \mathrm{div}\{\underline{u}(e+p)\} = 0 \tag{2.3}$$

and

$$e = \rho i + \tfrac{1}{2}\rho\underline{u}.\underline{u} \tag{2.4}$$

where

$$\rho = \rho(\underline{x},t)\ , \quad \underline{u} = \underline{u}(\underline{x},t) = \{u_1(\underline{x},t)\ ,\ u_2(\underline{x},t)\ ,\ u_3(\underline{x},t)\}^T\ ,$$

$$i = i(\underline{x},t)\ , \quad p = p(\underline{x},t) \quad \text{and} \quad e = e(\underline{x},t)$$

represent the density, velocity in the three co-ordinate directions, specific internal energy, pressure and total energy, respectively, at a general position $\underline{x} = (x_1,x_2,x_3)^T$ and at time t. We only consider the case of an ideal gas where the specific internal energy i is given by the equation of state

$$p = (\gamma-1)\rho i \tag{2.5}$$

and γ is the ratio of specific heat capacities of the fluid.

Consider a general orthogonal curvilinear co-ordinate system (x_1,x_2,x_3) where a line element $\underline{ds}$ is given by

$$\underline{ds} = h_1 dx_1 \hat{\underline{x}}_1 + h_2 dx_2 \hat{\underline{x}}_2 + h_3 dx_3 \hat{\underline{x}}_3$$

and $\hat{\underline{x}}_1,\hat{\underline{x}}_2,\hat{\underline{x}}_3$ are orthogonal.

The vector $\hat{\underline{x}}_i$ is of unit length and parallel to the co-ordinate lines with x_i increasing. Consider also a scalar field $\alpha = \alpha(x_1,x_2,x_3)$ a vector field

$$\underline{b} = \underline{b}(x_1,x_2,x_3) = b_1\hat{\underline{x}}_1 + b_2\hat{\underline{x}}_2 + b_3\hat{\underline{x}}_3 ,$$

and a 3×3 tensor $\underline{\underline{B}} = (B_{ij})$. Then the definitions of grad α, div $\underline{b}$ and div $\underline{\underline{B}}$ are as follows

$$\text{grad } \alpha = \frac{1}{h_1}\frac{\partial\alpha}{\partial x_1}\hat{\underline{x}}_1 + \frac{1}{h_2}\frac{\partial\alpha}{\partial x_2}\hat{\underline{x}}_2 + \frac{1}{h_3}\frac{\partial\alpha}{\partial x_3}\hat{\underline{x}}_3 \tag{2.6}$$

$$\text{div } \underline{b} = \left(\frac{1}{h_1h_2h_3}\frac{\partial}{\partial x_1}(h_2h_3b_1) + \frac{\partial}{\partial x_2}(h_1h_3b_2) + \frac{\partial}{\partial x_3}(h_1h_2b_3)\right) \tag{2.7}$$

and

$$(\text{div } \underline{\underline{B}})_i = \frac{1}{h_1h_2h_3}\left[\frac{\partial}{\partial x_1}(h_2h_3B_{1i}) + \frac{\partial}{\partial x_2}(h_1h_3B_{2i}) + \frac{\partial}{\partial x_3}(h_1h_2B_{3i})\right]$$

$$+ \frac{B_{ij}}{h_ih_j}\frac{\partial h_i}{\partial x_j} + \frac{B_{ki}}{h_ih_k}\frac{\partial h_i}{\partial x_k} - \frac{B_{ij}}{h_ih_j}\frac{\partial h_j}{\partial x_i} - \frac{B_{kk}}{h_ih_k}\frac{\partial h_k}{\partial x_i} \tag{2.8}$$

where (ijk) is a cyclic permutation of (123). If we use the expressions given by equations (2.6)-(2.8) in equations (2.1)-(2.5) together with

$$(\underline{\underline{uu}})_{ij} = u_iu_j$$

we obtain the following form for the Euler equations in an orthogonal curvilinear co-ordinate system:

$$\rho_t + \frac{1}{h_1h_2h_3}\left[\frac{\partial}{\partial x_1}(h_2h_3\rho u_1) + \frac{\partial}{\partial x_2}(h_1h_3\rho u_2) + \frac{\partial}{\partial x_3}(h_1h_2\rho u_3)\right] = 0 \tag{2.9}$$

$$(\rho u_i)_t + \frac{1}{h_1h_2h_3}\left[\frac{\partial}{\partial x_1}(h_2h_3\rho u_1u_i) + \frac{\partial}{\partial x_2}(h_1h_3\rho u_2u_i) + \frac{\partial}{\partial x_3}(h_1h_2\rho u_3u_i)\right]$$

$$+ \frac{\rho u_iu_j}{h_ih_j}\frac{\partial h_i}{\partial x_j} + \frac{\rho u_iu_k}{h_ih_k}\frac{\partial h_i}{\partial x_k} - \frac{\rho u_j^2}{h_ih_j}\frac{\partial h_j}{\partial x_i} - \frac{\rho u_k^2}{h_ih_k}\frac{\partial h_k}{\partial x_i} = -\frac{1}{h_i}\frac{\partial p}{\partial x_i}$$

$$i = 1,2,3 \qquad (2.10a\text{-}c)$$

and

$$e_t + \frac{1}{h_1h_2h_3}\left[\frac{\partial}{\partial x_1}\{h_2h_3u_1(e+p)\} + \frac{\partial}{\partial x_2}\{h_1h_3u_2(e+p)\} + \frac{\partial}{\partial x_3}\{h_1h_2u_3(e+p)\}\right]$$

$$= 0 \qquad (2.11)$$

where

$$e = \frac{p}{\gamma-1} + \tfrac{1}{2}\rho(u_1^2 + u_2^2 + u_3^2) \qquad (2.12)$$

and (ijk) is a cyclic permutation of (123).

If we now write

$$-\frac{1}{h_i}\frac{\partial p}{\partial x_i} = \frac{p}{h_1h_2h_3}\frac{\partial}{\partial x_i}(h_jh_k) - \frac{1}{h_1h_2h_3}\frac{\partial}{\partial x_i}(h_jh_kp)$$

$$i = 1,2,3$$

in equations (2.10a-c) then equations (2.9)-(2.12) can be written in vector form as

$$(h_1h_2h_3\underline{w})_t + \{h_2h_3\underline{f}(\underline{w})\}_{x_1} + \{h_1h_3\underline{g}(\underline{w})\}_{x_2}$$

$$+ \{h_1h_2\underline{h}(\underline{w})\}_{x_3} = \underline{r}_1 + \underline{r}_2 + \underline{r}_3 \qquad (2.13)$$

where

$$\underline{w} = (\rho, \rho u_1, \rho u_2, \rho u_3, e)^T \qquad (2.14)$$

$$\underline{w} = \frac{p}{\gamma-1} + \tfrac{1}{2}\rho q^2 \tag{2.15}$$

$$q^2 = u_1^2 + u_2^2 + u_3^2 \tag{2.16}$$

$$\underline{f}(\underline{w}) = (\rho u_1,\ p + \rho u_1^2,\ \rho u_1 u_2,\ \rho u_1 u_3,\ u_1(e+p))^T \tag{2.17}$$

$$\underline{g}(\underline{w}) = (\rho u_2,\ \rho u_2 u_1,\ p + \rho u_2^2,\ \rho u_2 u_3,\ u_2(e+p))^T \tag{2.18}$$

$$\underline{h}(\underline{w}) = (\rho u_3,\ \rho u_3 u_1,\ \rho u_3 u_2,\ p + \rho u_3,\ u_3(e+p))^T \tag{2.19}$$

and

$$\underline{r}_1 = \Big(0, p\frac{\partial}{\partial x_1}(h_2h_3) + \rho u_2^2 h_3 \frac{\partial h_2}{\partial x_1} + \rho u_3^2 h_2 \frac{\partial h_3}{\partial x_1},\ -\rho u_1 u_2 h_3 \frac{\partial h_2}{\partial x_1},\ -\rho u_1 u_3 h_2 \frac{\partial h_3}{\partial x_1},\ 0\Big)^T \tag{2.20}$$

$$\underline{r}_2 = \Big(0, -\rho u_2 u_1 h_3 \frac{\partial h_1}{\partial x_2},\ p\frac{\partial}{\partial x_2}(h_1h_3) + \rho u_3^2 h_1 \frac{\partial h_3}{\partial x_2} + \rho u_1^2 h_3 \frac{\partial h_1}{\partial x_2},\ -\rho u_2 u_3 h_1 \frac{\partial h_3}{\partial x_2},\ 0\Big)^T \tag{2.21}$$

$$\underline{r}_3 = \Big(0, -\rho u_3 u_1 h_2 \frac{\partial h_1}{\partial x_3},\ -\rho u_3 u_2 h_1 \frac{\partial h_2}{\partial x_3},\ p\frac{\partial}{\partial x_3}(h_1h_2) + \rho u_1^2 h_3 \frac{\partial h_1}{\partial x_2} + \rho u_2^2 h_1 \frac{\partial h_3}{\partial x_2},\ 0\Big)^T . \tag{2.22}$$

We have written the right hand side of equation (2.13) as the sum of three vectors $\underline{r}_i$ $i = 1,2,3$ where $\underline{r}_i$ has derivatives only with respect to x_i. This is done so that we can identify the terms in equation (2.13) with derivatives in one of the co-ordinate directions only.

In the next section we discuss a numerical technique for solving the equations of this section.

3. FLUX DIFFERENCE SPLITTING

In this section we consider a finite difference approximation for the solution of equations (2.13)-(2.22).

The finite difference approximation we propose is based on the approximate Riemann solver of Roe [1] (for the cartesian case), and the modification given by Glaister [2] for flows in one space dimension, sometimes referred to as duct flow.

We consider solving equations (2.13)-(2.22) using the technique of operator splitting. In particular, we propose solving the following equations along an x_1 coordinate line

$$(h_1 h_2 h_3 \underline{w})_t + (h_2 h_3 \underline{f}(w))_{x_1} = \underline{r}_1 \tag{3.1}$$

where

$$\underline{w} = (\rho, \rho u_1, \rho u_2, \rho u_3, e)^T \tag{3.2}$$

$$e = \frac{p}{\gamma - 1} + \tfrac{1}{2}\rho q^2 \tag{3.3}$$

$$q^2 = u_1^2 + u_2^2 + u_3^2 \tag{3.4}$$

and

$$\underline{r}_1 = \Big(0,\ p\frac{\partial}{\partial x_1}(h_2 h_3) + \rho u_2^2 h_3 \frac{\partial h_2}{\partial x_1} + u_3^2 h_2 \frac{\partial h_3}{\partial x_1},$$

$$- \rho u_1 u_2 h_3 \frac{\partial h_2}{\partial x_1},\ - \rho u_1 u_3 h_2 \frac{\partial h_3}{\partial x_1},\ 0\Big)^T . \tag{3.5}$$

(A similar analysis will follow for x_2 and x_3 coordinate lines.)

If we define a new variable $\underline{W} = h_2 h_3 \underline{w}$ and notice that $h_2 h_3 \underline{f}(\underline{w}) = \underline{f}(h_2 h_3 \underline{w}) = \underline{F}(\underline{W})$, then equation (3.1) can be rewritten in the form

$$(h_1 \underline{W})_t + (\underline{F}(\underline{W}))_{x_1} = \underline{r}_1(\underline{w}) . \tag{3.6}$$

This gives rise to new 'conserved' variables $\mathcal{R}$, M_1, M_2, M_3, E where $\mathcal{R} = h_2h_3\rho$, $M_1 = h_2h_3m_1$, $M_2 = h_2h_3m_2$, $M_3 = h_2h_3m_3$ and $E = h_2h_3e$. (Here m_1, m_2, m_3 denote the components of the momentum in the $\hat{x}_1$, $\hat{x}_2$, $\hat{x}_3$ directions, respectively. It also gives a new 'pressure' variable $P = h_2h_3p$. Quantities with the dimension of velocity are unaltered, e.g. the components of the velocity $u_1 = U_1$, $u_2 = U_2$, $u_3 = U_3$, sound speed $a = \sqrt{\frac{\gamma p}{\rho}} = \sqrt{\frac{\gamma P}{\mathcal{R}}}$ and enthalpy $h = (e+p)/\rho = (E+P)/\mathcal{R} = H$. In particular the matrix $A = \frac{\partial \underline{F}}{\partial \underline{W}}(\underline{W})$ involves only velocities and is the same as $\frac{\partial \underline{f}}{\partial \underline{w}}(\underline{w})$.

Using these new variables equations (3.1)-(3.5) become

$$\begin{bmatrix} h_1\,\mathcal{R} \\ h_1\,\mathcal{R}\,U_1 \\ h_1\,\mathcal{R}\,U_2 \\ h_1\,\mathcal{R}\,U_3 \\ h_1\,E \end{bmatrix}_t + \begin{bmatrix} \mathcal{R}\,U_1 \\ P + \mathcal{R}\,U_1^2 \\ \mathcal{R}\,U_1U_2 \\ \mathcal{R}\,U_1U_3 \\ U_1(E+P) \end{bmatrix}_{x_1} = \underline{r}_1 \tag{3.7}$$

where

$$E = \frac{P}{\gamma-1} + \tfrac{1}{2}\mathcal{R}Q^2 \tag{3.8}$$

$$Q^2 = U_1^2 + U_2^2 + U_3^2 \quad . \tag{3.9}$$

We now propose a finite difference algorithm for the solution of equations (3.7)-(3.9) by noting their similarity to the cartesian case $h_1 = h_2 = h_3 = 1$, i.e.

$$\begin{bmatrix} \rho \\ \rho\,u_1 \\ \rho\,u_2 \\ \rho\,u_3 \\ e \end{bmatrix} + \begin{bmatrix} \rho\,u_1 \\ p + \rho\,u_1^2 \\ \rho\,u_1u_2 \\ \rho\,u_1u_3 \\ u_1(e+p) \end{bmatrix}_{x_1} = \underline{0} \tag{3.10}$$

where

$$e = \frac{p}{\gamma-1} + \tfrac{1}{2}\rho q^2 \tag{3.11}$$

$$q^2 = u_1^2 + u_2^2 + u_3^2 \quad . \tag{3.12}$$

We consider a fixed grid in space and time with grid sizes Δx_1, Δt, respectively, and label the points on an x_1-coordinate line so that $x_{1_j} = x_{1_{j-1}} + \Delta x_1$, and on the t-axis $t_n = t_{n-1} + \Delta t$. $\underline{W}_j^n$, $\underline{w}_j^n$ denote the approximations to $\underline{W}(x_{1_j},x_{2_0},x_{3_0},t_n)$, $\underline{w}(x_{1_j},x_{2_0},x_{3_0},t_n)$ respectively. We also use the notation that on an x_1-coordinate line the coordinates x_2,x_3 will take the constant values x_{2_0},x_{3_0}, respectively.

Using the relationship $\underline{W}(x_{1_j},x_{2_0},x_{3_0},t_n) = h_2h_3\underline{w}(x_{1_j},x_{2_0},x_{3_0},t_n)$, we may write

$$\underline{W}_j^n = \hat{h}_j^{23}\ \underline{w}_j^n$$

where $\hat{h}_j^{23}$ represents an average value of h_2h_3. Assuming that at any time $t_n = n\Delta t$, $\underline{W}_j^n$ represents a piecewise constant approximation to $\underline{W}(x_{1_j},x_{2_0},x_{3_0},t_n)$ in the interval $(x_{1_j} - \Delta x_1/2, x_{1_j} + \Delta x_1/2)$ (as in the usual Godunov approach), $\hat{h}_j^{23}$ is given by the integral

$$\hat{h}_j^{23} = \frac{1}{\Delta x_1}\int_{x_{1_j}-\Delta x_1/2}^{x_{1_j}+\Delta x_1/2} h_2(x_1,x_{2_0},x_{3_0})h_3(x_1,x_{2_0},x_{3_0})\,dx_1 \quad . \tag{3.14}$$

We can then recover the approximation $\underline{w}_j^n$ to $\underline{w}(x_{1_j},x_{2_0},x_{3_0},t_n)$ at time $t = t_n$ from equation (3.13), i.e.

$$\underline{w}_j^n = \underline{W}_j^n \,/\, \hat{h}_j^{23} \quad . \tag{3.15}$$

Consider the interval $[x_{1_{j-1}}, x_{1_j}]$ and denote by $\underline{W}_L$, $\underline{W}_R$ the approximations to $\underline{W}$ at $x_{1_{j-1}}, x_{1_j}$ respectively. We now rewrite equation (3.6) as

$$(h_1\underline{W})_t + \frac{\partial \underline{F}}{\partial \underline{W}}(\underline{W})\underline{W}_{x_1} = \underline{r}_1(\underline{w}) \tag{3.16}$$

and solve the associated one-dimensional Riemann problem

$$(h_1\underline{W})_t + \tilde{\underline{A}}(\underline{W}_L, \underline{W}_R)\underline{W}_{x_1} = \underline{r}_1(\underline{w}) \tag{3.17}$$

with data $\underline{W}_L, \underline{W}_R$ either side of the point $x_{1_{j-\frac{1}{2}}}$, linearising $\underline{A}$ in the form $\tilde{\underline{A}}(\underline{W}_L, \underline{W}_R)$ which is then taken to be a constant matrix (see below). We shall use the approximate form of equation (3.17),

$$\hat{h}_{1_{j-\frac{1}{2}}} \frac{(\underline{W}_P^{n+1} - \underline{W}_P^n)}{\Delta t} + \tilde{\underline{A}}(\underline{W}_L, \underline{W}_R) \frac{(\underline{W}_R - \underline{W}_L)}{\Delta x_1} = \hat{\underline{r}}_1(\underline{w}^n) \tag{3.18}$$

where $\tilde{\underline{A}}(\underline{W}_L, \underline{W}_R)$ is the Roe matrix (3.20),

$$\hat{h}_{1_{j-\frac{1}{2}}} = \frac{1}{\Delta x_1} \int_{x_{1_{j-1}}}^{x_{1_j}} h_1(x_1, x_{2_0}, x_{3_0})\, dx_1$$

$\hat{\underline{r}}_1$ is an approximation to $\underline{r}_1$ and P may be L or R.

The Roe matrix $\tilde{\underline{A}}(\underline{W}_L, \underline{W}_R)$ is an approximation to the Jacobian $\underline{A} = \frac{\partial \underline{F}}{\partial \underline{W}}(\underline{W})$ and because of the remarks following equation (3.6) it can be seen that

$$\tilde{\underline{A}}(\underline{W}_L, \underline{W}_R) = \tilde{\underline{A}}(\underline{w}_L, \underline{w}_R) \tag{3.19}$$

where the Roe matrix $\tilde{\underline{A}}(\underline{w}_L, \underline{w}_R)$ is an approximation to $\frac{\partial \underline{f}}{\partial \underline{w}}(\underline{w})$.

The Roe matrix is constructed so that $\underline{f}_R - \underline{f}_L = \tilde{\underline{A}}(\underline{w}_L, \underline{w}_R)(\underline{w}_R - \underline{w}_L)$ for any finite change of state and is given [1] by

$$\tilde{A} = \begin{bmatrix} 0 & 1 & 0 & 0 & 0 \\ \frac{(\gamma-1)}{2}\tilde{Q}^2-\tilde{u}_1^2 & (3-\gamma)\tilde{u}_1 & -(\gamma-1)\tilde{u}_2 & -(\gamma-1)\tilde{u}_3 & \gamma-1 \\ -\tilde{u}_1\tilde{u}_2 & \tilde{u}_2 & \tilde{u}_1 & 0 & 0 \\ -\tilde{u}_1\tilde{u}_3 & \tilde{u}_3 & 0 & \tilde{u}_1 & 0 \\ \frac{(\gamma-1)}{2}\tilde{u}_1\tilde{Q}^2-\tilde{u}_1\tilde{H} & \tilde{H}-(\gamma-1)\tilde{u}_1^2 & -(\gamma-1)\tilde{u}_1\tilde{u}_2 & -(\gamma-1)\tilde{u}_1\tilde{u}_3 & \gamma\tilde{u}_1 \end{bmatrix} \tag{3.20}$$

where $\tilde{Y}$ denotes a square root mean of left and right states of Y, namely,

$$Y = \frac{\sqrt{R_L}\,Y_L + \sqrt{R_R}\,Y_R}{\sqrt{R_L} + \sqrt{R_R}} \tag{3.21}$$

for all variables other than R and ρ, and

$$\tilde{Q}^2 = \tilde{u}_1^2 + \tilde{u}_2^2 + \tilde{u}_3^2 \ . \tag{3.22}$$

In later analysis we need mean values for R and ρ, given by

$$\tilde{R} = \sqrt{R_L R_R}\ , \qquad \tilde{\rho} = \sqrt{\rho_L \rho_R}\ . \tag{3.23}$$

The eigenvalues of $\tilde{A}$ are

$$\tilde{\lambda}_1 = \tilde{u}_1 + \tilde{a}\ , \qquad \tilde{\lambda}_2 = \tilde{u}_1 - \tilde{a}\ , \qquad \tilde{\lambda}_{3,4,5} = \tilde{u}_1 \tag{3.24}$$

with corresponding eigenvectors

$$\begin{aligned} \tilde{e}_1 &= (1,\ \tilde{u}_1 + \tilde{a},\ \tilde{u}_2,\ \tilde{u}_3,\ \tilde{H} + \tilde{u}_1\tilde{a})^T \\ \tilde{e}_2 &= (1,\ \tilde{u}_1 - \tilde{a},\ \tilde{u}_2,\ \tilde{u}_3,\ \tilde{H} - \tilde{u}_1\tilde{a})^T \\ \tilde{e}_3 &= (1,\ \tilde{u}_1,\ \tilde{u}_2,\ \tilde{u}_3,\ \tfrac{1}{2}\tilde{Q}^2)^T \\ \tilde{e}_4 &= (0,\ 0,\ \tilde{u}_2,\ 0,\ \tilde{u}_2^2)^T \\ \tilde{e}_5 &= (0,\ 0,\ 0,\ \tilde{u}_3,\ \tilde{u}_3^2)^T \end{aligned} \tag{3.25a-e}$$

(as in the standard cartesian case when $h_1 = h_2 = h_3 = 1$), where $\tilde{H}$ is calculated using equation (3.21) and the mean sound speed $\tilde{a}$ is calculated from

$$\tilde{a}^2 = (\gamma-1)(\tilde{H} - \tfrac{1}{2}Q^2) \quad . \tag{3.26}$$

Using the above properties of $\tilde{A}$ we can write equation (3.17) as

$$\hat{h}_{1_{j-\frac{1}{2}}} \frac{(\underline{W}_P^{n+1} - \underline{W}_P^n)}{\Delta t} + \frac{\underline{F}_R - \underline{F}_L}{\Delta x_1} = \hat{\underline{r}}_1(\underline{w}^n) \tag{3.27}$$

where $\hat{\underline{r}}_1(\underline{w}^n)$ is a suitable approximation to the term $\underline{r}_1(\underline{w})$ on the right hand side of equation (3.17). We thus obtain

$$\hat{h}_{1_{j-\frac{1}{2}}} (\underline{W}_P^{n+1} - \underline{W}_P^n) = \Delta t \hat{\underline{r}}_1(\underline{w}^n) - \frac{\Delta t}{\Delta x_1} (\underline{F}_R - \underline{F}_L) \quad . \tag{3.28}$$

Before we describe the mechanism to update $\underline{W}_j^n$ to $\underline{W}_j^{n+1}$ along the x_1-coordinate line we look at the approximation $\hat{\underline{r}}_1(\underline{w}^n)$ used for $\underline{r}_1(\underline{w})$.

Now,

$$\underline{r}_1(\underline{w}) = \Big(0, \frac{P}{h_2h_3}\frac{\partial}{\partial x_1}(h_2h_3) + \frac{\rho u_2^2}{h_2}\frac{\partial}{\partial x_1}h_2 + \frac{\rho u_3^2}{h_3}\frac{\partial}{\partial x_1}h_3 ,$$

$$- \frac{\rho u_1 u_2}{h_2}\frac{\partial}{\partial x_1}h_2, - \frac{\rho u_1 u_3}{h_3}\frac{\partial}{\partial x_1}h_3, 0\Big)^T \tag{3.29}$$

and using the change of variable $\underline{W} = h_2h_3\underline{w}$, we obtain

$$\underline{r}_1 = \Big(0, P\frac{\partial}{\partial x_1}\log_e(h_2h_3) + \rho u_2^2\frac{\partial}{\partial x_1}\log_e h_2 + \rho u_3^2\frac{\partial}{\partial x_1}\log_e h_3 ,$$

$$- \rho u_1 u_2\frac{\partial}{\partial x_1}\log_e h_2, - \rho u_1 u_3\frac{\partial}{\partial x_1}\log_e h_3, 0\Big)^T \quad . \tag{3.30}$$

Note that we need only to approximate the second, third and fourth components. For the second component we notice first that, since the sound speed a is given by $a^2 = \frac{\gamma p}{\rho} = \frac{\gamma P}{R}$, we may write

$$(\underline{r}_1)_2 = \frac{Ra^2}{\gamma}\frac{\partial}{\partial x_1}\log_e(h_2h_3) + Ru_2^2\frac{\partial}{\partial x_1}\log_e h_2 + Ru_3^2\frac{\partial}{\partial x_1}\log_e h_3 \tag{3.31}$$

and approximate $(\underline{r}_1)_2$ by $(\hat{\underline{r}}_1)_2$ where

$$(\hat{\underline{r}}_1)_2 = \frac{\tilde{R}\tilde{a}^2}{\gamma}\frac{\Delta_1(\log_e(h_2h_3))}{\Delta x_1} + \tilde{\tilde{R}}\tilde{u}_2^2\frac{\Delta_1(\log_e h_2)}{\Delta x_1} + \tilde{\tilde{R}}\tilde{u}_3^2\frac{\Delta_1(\log_e h_3)}{\Delta x_1} \tag{3.32}$$

and

$$\Delta_1 f(x_1,x_2,x_3) = f(x_{1_j},x_{2_0},x_{3_0}) - f(x_{1_{j-1}},x_{2_0},x_{3_0}) . \tag{3.33}$$

Similarly, we approximate $(\underline{r}_1)_3$, $(\underline{r}_1)_4$ by $(\tilde{\underline{r}}_1)_3$, $(\tilde{\underline{r}}_1)_4$ where

$$(\hat{\underline{r}}_1)_3 = -\tilde{\tilde{R}}\tilde{u}_1\tilde{u}_2\Delta_1(\log_e h_2) \tag{3.34}$$

$$(\hat{\underline{r}}_1)_4 = -\tilde{\tilde{R}}\tilde{u}_1\tilde{u}_3\Delta_1(\log_e h_3) . \tag{3.35}$$

In the cartesian case the procedure [1] is to project $\Delta\underline{f} = \underline{f}_R - \underline{f}_L$ onto the eigenvectors of $\tilde{A}$. Each projection represents the contribution of one wave system to $\Delta\underline{f}$. Here we follow a suggestion of Roe [3] for the one-dimensional case of duct flow, and find the projections both of $\Delta\underline{F} = \underline{F}_R - \underline{F}_L$ and also $\hat{\underline{r}}_1(\underline{w}^n)$. We than update $\underline{w}_j^n$ to $\underline{w}_j^{n+1}$ as follows.

Suppose

$$\Delta\underline{w} = \underline{w}_R - \underline{w}_L = \sum_{i=1}^{5}\tilde{\alpha}_i\tilde{\underline{e}}_i \tag{3.36}$$

so that

$$\Delta\underline{F} = \underline{F}_R - \underline{F}_L = \sum_{i=1}^{5}\tilde{\lambda}_i\tilde{\alpha}_i\tilde{\underline{e}}_i . \tag{3.37}$$

Since $\tilde{A}$ has eigenvalues $\tilde{\lambda}_i$ with corresponding eigenvectors $\tilde{\underline{e}}_i$ and

$$\hat{\underline{r}}_1(\underline{w}^n) = -\frac{1}{\Delta x_1}\sum_{i=1}^{5}\tilde{\beta}_i\tilde{\underline{e}}_i \tag{3.38}$$

we may rewrite equations (3.28) as

$$\underline{W}_P^{n+1} = \underline{W}_P^n - \frac{\Delta t}{\hat{h}_{1_{j-\frac{1}{2}}}\Delta x_1}\sum_{i=1}^{5}\tilde{\lambda}_i\tilde{\gamma}_i\tilde{\underline{e}}_i \tag{3.39}$$

where

$$\tilde{\gamma}_i = \tilde{\alpha}_i + \tilde{\beta}_{i/\tilde{\lambda}_i} \tag{3.40}$$

and P may be L or R . To update $\underline{W}^n$ to $\underline{W}^{n+1}$ we apply a sequence of one dimensional calculations along computational grid lines in the x_1,x_2 and x_3-directions in turn. The algorithm along the x_1-coordinate line where $x_2 = x_{2_0}$, $x_3 = x_{3_0}$ uses first order upwind differencing, i.e. for each cell $[x_{1_{j-1}},x_{1_j}]$ we add $-\frac{\Delta t\tilde{\lambda}_i\tilde{\gamma}_i\tilde{\underline{e}}_i}{\Delta x_1\hat{h}_{1_{j-\frac{1}{2}}}}$ to $\underline{W}_j^n$ when $\tilde{\lambda}_i > 0$ and $-\frac{\Delta t\tilde{\lambda}_i\tilde{\gamma}_i\tilde{\underline{e}}_i}{\Delta x_1\hat{h}_{1_{j-\frac{1}{2}}}}$ to $\underline{W}_{j-1}^n$ when $\tilde{\lambda}_i < 0$ (see figure 1).

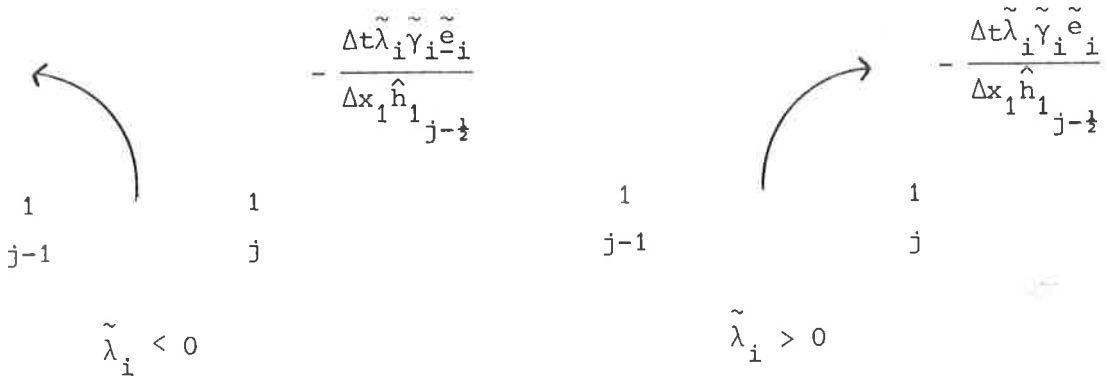

Figure 1

If we follow the algebra through, we obtain

$$\tilde{\alpha}_1 = \frac{1}{2\tilde{a}^2}(\Delta P + \tilde{R}\tilde{a}\Delta U_1) \tag{3.41a}$$

$$\tilde{\alpha}_2 = \frac{1}{2\tilde{a}^2}(\Delta P - \tilde{R}\tilde{a}\Delta U_1) \tag{3.41b}$$

$$\tilde{\alpha}_3 = \Delta R - \frac{\Delta P}{\tilde{a}^2} \tag{3.41c}$$

$$\tilde{\alpha}_4 = \frac{\tilde{R}}{\tilde{U}_2}\Delta U_2 \tag{3.41d}$$

$$\tilde{\alpha}_5 = \frac{\tilde{R}}{\tilde{U}_3}\Delta U_3 \tag{3.41e}$$

$$\tilde{\beta}_1 = -\frac{1}{2\tilde{a}^2}\left[(\gamma-1)\left(\tilde{U}_1(\hat{\underline{r}}_1)_2 + \tilde{U}_2(\hat{\underline{r}}_1)_3\right) + \tilde{U}_3(\hat{\underline{r}}_1)_4\right) - \tilde{a}(\hat{\underline{r}}_1)_2\Big] \tag{3.42a}$$

$$\tilde{\beta}_2 = -\frac{1}{2\tilde{a}^2}\left[(\gamma-1)\left(\tilde{U}_1(\hat{\underline{r}}_1)_2 + \tilde{U}_2(\hat{\underline{r}}_1)_3 + \tilde{U}_3(\hat{\underline{r}}_1)_4\right) + \tilde{a}(\hat{\underline{r}}_1)_2\Big] \tag{3.42b}$$

$$\tilde{\beta}_3 = \frac{(\gamma-1)}{\tilde{a}^2}\left(\tilde{U}_1(\hat{\underline{r}}_1)_2 + \tilde{U}_2(\hat{\underline{r}}_1)_3 + \tilde{U}_3(\hat{\underline{r}}_1)_4\right) \tag{3.42c}$$

$$\tilde{\beta}_4 = (\hat{\underline{r}}_1)_3/\tilde{U}_2 \tag{3.42d}$$

$$\tilde{\beta}_5 = (\hat{\underline{r}}_1)_4/\tilde{U}_3 \tag{3.42e}$$

and $(\hat{\underline{r}}_1)_2$, $(\hat{\underline{r}}_1)_3$, $(\hat{\underline{r}}_1)_4$ are given by equations (3.32)-(3.35).

A similar analysis will follow for updating the solution in the x_2 and x_3 coordinate directions. In particular, for a given geometry many of the expressions we have derived will be greatly simplified: however, we must take account of the computational mesh

that results. In addition to the increments given here, we can calculate second order corrections by transferring fractions of the increments described in figure 1 (see [4,5,6]). If we limit these transfers using a suitable flux limiter or B-function (see [4,5,6]), the scalar scheme will be second order almost everywhere, oscillation free, and will sharpen up certain features that would be smeared by using the first order method only.

In the next section we give the Euler equations for axially symmetric flow, and show how the algorithm of this section simplifies in this case.

4. AXIALLY SYMMETRIC FLOW

In this section we describe the algorithm of §3 as applied to the case of axially symmetric flow.

The Euler equations for flows dependent only on R, z and t, (independent of ϕ), where R, ϕ, z denote a cylindrical coordinate system may be written in the form

$$\begin{pmatrix} \rho \\ \rho u \\ \rho v \\ e \end{pmatrix}_t + \frac{1}{R}\begin{pmatrix} R\rho u \\ R\rho u^2 \\ R\rho uv \\ Ru(e+p) \end{pmatrix}_R + \begin{pmatrix} \rho v \\ \rho uv \\ \rho v^2 \\ v(e+p) \end{pmatrix}_z = \begin{pmatrix} 0 \\ -p_R \\ 0 \\ 0 \end{pmatrix} \tag{4.1}$$

where

$$e = \frac{p}{\gamma-1} + \tfrac{1}{2}\rho(u^2 + v^2) \quad . \tag{4.2}$$

The flow variables ρ, u, v, p depend on (R,z,t) where $R = \sqrt{x^2+y^2}$ is the radial coordinate and (x,y,z) are cartesian coordinates. The velocity components in the directions R,z increasing are u,v, respectively, and the velocity component in the direction ϕ increasing is set to zero.

Equations (4.1)-(4.2) can be rewritten using the change of variable $\underline{W} = R\underline{w}$, as

$$\underline{W}_t + \underline{F}(\underline{W})_R + \underline{H}(\underline{W})_z = \underline{g}(\underline{w}) \tag{4.3}$$

where

$$\underline{W} = (R,\ RU,\ RV,\ E)^T \tag{4.4}$$

$$\underline{F}(\underline{W}) = (RU,\ P+RU^2,\ RUV,\ U(E+P))^T \tag{4.5}$$

$$\underline{H}(\underline{W}) = (RV,\ RUV,\ P+RV^2,\ V(E+P))^T \tag{4.6}$$

and

$$\underline{g}(\underline{w}) = (0,\ p\frac{\partial}{\partial R}(R),\ 0,\ 0)^T \quad . \tag{4.7}$$

The variables $\bar{R}$, P, E are given by $\bar{R} = R\rho$, $P = Rp$, $E = Re$. Those variables with the dimensions of velocity, however, remain unchanged, i.e. $U = u$, $V = v$, the enthalpy $H = (E+P)/\bar{R} = (e+p)/\rho = h$, and the sound speed $a = \sqrt{\frac{\gamma p}{\rho}} = \sqrt{\frac{\gamma P}{\bar{R}}}$. We leave the term $\frac{\partial}{\partial R}(R)$ in equation (4.7) since it indicates that this term should be incorporated in the one dimensional algorithm in the R direction, i.e. along a line z = constant.

The algorithm of §3 as applied to equations (4.1)-(4.2) can be described as follows.

Consider a fixed grid in space and time, with grid sizes ΔR, Δz and Δt, respectively, and label the points on an R-coordinate line so that $R_j = R_{j-1} + \Delta R$, on a z-coordinate line so that $z_j = z_{j-1} + \Delta z$, and let $t_n = t_{n-1} + \Delta t$ as usual. This gives rise to a computational mesh that is rectangular in the R-z plane. We assume that at any time $t_n = n\Delta t$, $\underline{W}_j^n$, $\underline{w}_j^n$ represent approximations to $\underline{W}(R_j, z_0, t_n)$, $\underline{w}(R_j, z_0, t_n)$, respectively, on an R-coordinate line $(z = z_0)$, or $\underline{W}(R_0, z_j, t_n)$, $\underline{w}(R_0, z_j, t_n)$, respectively, on a z-coordinate line $(R = R_0)$. We therefore have the relationship

$$\underline{W}_j^n = \hat{R}\,\underline{w}_j^n \tag{4.8}$$

where

$$\hat{R} = \frac{1}{\Delta R}\int_{R_j-\Delta R/2}^{R_j+\Delta R/2} R\,dR \tag{4.9a}$$

on an R-coordinate line $z = z_0$, or

$$\hat{R} = \frac{1}{\Delta z} \int_{z_j - \Delta z/2}^{z_j + \Delta z/2} R_0 \, dR \tag{4.9b}$$

on a z-coordinate line $R = R_0$. Performing the integration in equations (4.9a-b) yields

$$\underline{W}_j^n = R_j \underline{w}_j^n \tag{4.10a}$$

or

$$\underline{W}_j^n = R_0 \underline{W}_j^n \tag{4.10b}$$

on R,z-coordinate lines $z = z_0$, $R = R_0$, respectively. (N.B. The change of variable $\underline{W} = R\underline{w}$ is applicable to the one dimensional operators in both the R and z directions, and this is highlighted by the results given by equations (4.10a-b).

The approximate solution of equations (4.1)-(4.2) can now be found by using the one-dimensional algorithm of §3 and incorporating the technique of operator splitting. Along an R-coordinate line ($z = z_0$), for each cell $[R_{j-1}, R_j]$ we

$$\text{add } -\frac{\Delta t}{\Delta R} \tilde{\lambda}_i^R \tilde{\gamma}_i^R \underline{e}_{i-i} \text{ to } \underline{W}_j^n \text{ when } \tilde{\lambda}_i^R > 0$$

and

$$\text{add } -\frac{\Delta t}{\Delta R} \tilde{\lambda}_i^R \tilde{\gamma}_i^R \underline{e}_{i-i} \text{ to } \underline{W}_{j-1}^n \text{ when } \tilde{\lambda}_i^R < 0$$

where

$$\tilde{\gamma}_i^R = \tilde{\alpha}_i^R + \tilde{\beta}_i^R / \tilde{\lambda}_i^R \tag{4.11}$$

$$\tilde{\alpha}_1^R = \frac{1}{2\tilde{a}^2} (\Delta P + \tilde{\tilde{R}} \tilde{a} \Delta U) \tag{4.12a}$$

$$\tilde{\alpha}_2^R = \frac{1}{2\tilde{a}^2} (\Delta P - \tilde{\tilde{R}} \tilde{a} \Delta U) \tag{4.12b}$$

$$\tilde{\alpha}_3^R = \Delta R - \Delta P / \tilde{a}^2 \tag{4.12c}$$

$$\tilde{\alpha}_4^R = \frac{\tilde{R}}{\tilde{V}} \Delta V \tag{4.12d}$$

$$\tilde{\lambda}_1^R = \tilde{U} + \tilde{a} \tag{4.13a}$$

$$\tilde{\lambda}_2^R = \tilde{U} - \tilde{a} \tag{4.13b}$$

$$\tilde{\lambda}_3^R = \tilde{U} \tag{4.13c}$$

$$\tilde{\lambda}_4^R = \tilde{U} \tag{4.13d}$$

$$\tilde{\beta}_1^R = \frac{\Delta R \hat{g}_2}{2\tilde{a}^2} (\tilde{a} + (\gamma-1)\tilde{U}) \tag{4.14a}$$

$$\tilde{\beta}_2^R = -\frac{\Delta R \hat{g}_2}{2\tilde{a}^2} (\tilde{a} - (\gamma-1)\tilde{U}) \tag{4.14b}$$

$$\tilde{\beta}_3^R = -\frac{\Delta R \hat{g}_2}{\tilde{a}^2} (\gamma-1)\tilde{U} \tag{4.14c}$$

$$\tilde{\beta}_4^R = 0 \tag{4.14d}$$

and

$$\underset{\sim}{\tilde{e}}_1^R = (1, \tilde{U} + \tilde{a}, \tilde{V}, \tilde{H} + \tilde{U}\tilde{a})^T \tag{4.15a}$$

$$\underset{\sim}{\tilde{e}}_2^R = (1, \tilde{U} - \tilde{a}, \tilde{V}, \tilde{H} - \tilde{U}\tilde{a})^T \tag{4.15b}$$

$$\underset{\sim}{\tilde{e}}_3^R = (1, \tilde{U}, \tilde{V}, \tfrac{1}{2}(\tilde{U}^2 + \tilde{V}^2))^T \tag{4.15d}$$

$$\underset{\sim}{\tilde{e}}_4^R = (0, 0, \tilde{V}, \tilde{V}^2)^T \quad .$$

The averages $\tilde{U}$, $\tilde{V}$, $\tilde{H}$ are defined as

$$\tilde{Y} = \frac{\sqrt{R_{j-1}}\, Y_{j-1} + \sqrt{R_j}\, Y_j}{\sqrt{R_{j-1}} + \sqrt{R_j}}, \qquad Y = U,V,H, \tag{4.16}$$

$\tilde{R}$, $\tilde{a}$ are given by

$$\tilde{R} = \sqrt{R_{j-1}R_j} \tag{4.17}$$

$$\tilde{a}^2 = (\gamma-1)\{\tilde{H} - \tfrac{1}{2}(\tilde{U}^2 + \tilde{V}^2)\} \tag{4.18}$$

and the difference Δf is defined by

$$\Delta f = f_j - f_{j-1} \quad . \tag{4.19}$$

The coefficients $\tilde{\beta}_i$ here have been determined by setting

$$-\frac{1}{\Delta R}\sum_{i=1}^{4}\tilde{\beta}_i\tilde{R}\tilde{e}_{i-i}^{R} = \begin{pmatrix} 0 \\ \hat{g}_2 \\ 0 \\ 0 \end{pmatrix} \tag{4.20}$$

and choosing a suitable approximation $\hat{g}_2$ to the term $g_2 = P\frac{\partial}{\partial R}(R)$ of equation (4.7).

We write $g_2 = \frac{\rho a^2}{\gamma}\frac{\partial}{\partial R}(R)$ and approximate

$$\hat{g}_2 = \frac{\tilde{\rho}\tilde{a}^2}{\gamma}\frac{\Delta(R)}{\Delta R} = \frac{\tilde{\rho}\tilde{a}^2}{\gamma} \quad , \tag{4.21}$$

where $\tilde{\rho} = \sqrt{\rho_{j-1}\rho_j}$ as in the cartesian case.

Finally, we note that

$$\tilde{\rho} = \sqrt{\rho_{j-1}\rho_j} = \sqrt{\frac{R_{j-1}}{\hat{R}_{j-1}}\frac{R_j}{\hat{R}_j}} = \frac{\tilde{R}}{\tilde{\tilde{R}}} \tag{4.22}$$

where

$$\tilde{R} = \sqrt{\hat{R}_{j-1}\hat{R}_j} = \sqrt{R_{j-1}R_j} \text{ is averaged}$$

in the same way as ρ , R . Therefore

$$\hat{g}_2 = \frac{\tilde{\tilde{R}}\tilde{a}^2}{\tilde{R}\gamma} \tag{4.23}$$

and $\tilde{\beta}_1^R$, $\tilde{\beta}_2^R$, $\tilde{\beta}_3^R$, $\tilde{\beta}_4^R$ are given by

$$\tilde{\beta}_1^R = \frac{\tilde{R}\Delta R}{2\gamma\tilde{R}}(\tilde{a} + (\gamma-1)\tilde{U}) \tag{4.24a}$$

$$\tilde{\beta}_2^R = -\frac{\tilde{R}\Delta R}{2\gamma\tilde{R}}(\tilde{a} - (\gamma-1)\tilde{U}) \tag{4.24b}$$

$$\tilde{\beta}_3^R = -\frac{\tilde{R}\Delta R}{\gamma\tilde{R}}(\gamma-1)U \tag{4.24c}$$

$$\tilde{\beta}_4^R = 0 \quad . \tag{4.24d}$$

The algorithm for updating the solution along a z-coordinate line $(R = R_0)$ is as follows. For each cell $[z_{j-1}, z_j]$ we add $-\frac{\Delta t}{\Delta z}\tilde{\lambda}_i^z\tilde{\alpha}_i^z\tilde{e}_{i-i}^z$ to $\underset{-}{W}_j^n$ when $\tilde{\lambda}_i^z > 0$ and add $-\frac{\Delta t}{\Delta z}\tilde{\lambda}^z\tilde{\alpha}^z\tilde{e}_{-i}^z$ to $\underset{-}{W}_{j-1}^n$ when $\tilde{\lambda}_i^z < 0$ where

$$\tilde{\alpha}_1^z = \frac{1}{2\tilde{a}^2}(\Delta P + \tilde{\tilde{R}}\tilde{a}\Delta V) \tag{4.25a}$$

$$\tilde{\alpha}_2^z = \frac{1}{2\tilde{a}^2}(\Delta P - \tilde{\tilde{R}}\tilde{a}\Delta V) \tag{4.25b}$$

$$\tilde{\alpha}_3^z = \Delta R - \Delta P/\tilde{a}^2 \tag{4.25c}$$

$$\tilde{\alpha}_4^z = \frac{\tilde{R}}{U}\Delta U \tag{4.25d}$$

$$\tilde{\lambda}_1^z = \tilde{v} + \tilde{a} \tag{4.26a}$$

$$\tilde{\lambda}_2^z = \tilde{v} - \tilde{a} \tag{4.26b}$$

$$\tilde{\lambda}_3^z = \tilde{V} \tag{4.26c}$$

$$\tilde{\lambda}_4^z = \tilde{V} \tag{4.26d}$$

and

$$\tilde{\underline{e}}_1^z = (1,\ \tilde{V} + \tilde{a},\ \tilde{U},\ \tilde{H} + \tilde{V}\tilde{a})^T \tag{4.27a}$$

$$\tilde{\underline{e}}_2^z = (1,\ \tilde{V} - \tilde{a},\ \tilde{U},\ \tilde{H} - \tilde{V}\tilde{a})^T \tag{4.27b}$$

$$\tilde{\underline{e}}_3^z = \left(1,\ \tilde{V},\ \tilde{U},\ \tfrac{1}{2}(\tilde{U}^2 + \tilde{V}^2)\right)^T \tag{4.27c}$$

$$\tilde{\underline{e}}_4^z = (0,\ 0,\ \tilde{U},\ \tilde{U}^2)^T \quad . \tag{4.27d}$$

The averages $\tilde{U}$, $\tilde{V}$, $\tilde{H}$, $\tilde{R}$, $\tilde{a}$ are defined as in equations (4.16)-(4.18) and the difference Δf is given by equation (4.19). We note that in this case $\tilde{\beta}_1^z = \tilde{\beta}_2^z = \tilde{\beta}_3^z = \tilde{\beta}_4^z = 0$.

Summarising, we project the initial data $\underline{w}(R,z,0)$ onto a set of piecewise constant states $\underline{W}_{ij}^o = R_i \underline{w}(R_i, z_j, 0)$ on the rectangle

$$(R_i - \Delta R/2,\ R_i + \Delta R/2) \times (z_j - \Delta z/2,\ z_j + \Delta z/2) ,$$

march forward to a time $2m\Delta t$ using a time step Δt by sweeping m times in the R and z-directions alternately as described by equations (4.8)-(4.27d), and recover the approximate solution using

$$\underline{w}_{ij}^{2m\Delta t} = \underline{W}_{ij}^{2m\Delta t}/R_i \ .$$

In the next section we describe two test problems that can be used to test the algorithm of this section.

5. NUMERICAL RESULTS

In this section we describe two test problems that can be used to test the algorithm of §4 and display the numerical results obtained.

Problem 1

This problem begins with uniform Mach 3 flow in a cylindrical tunnel containing a cylindrical step, (see Figure 2).

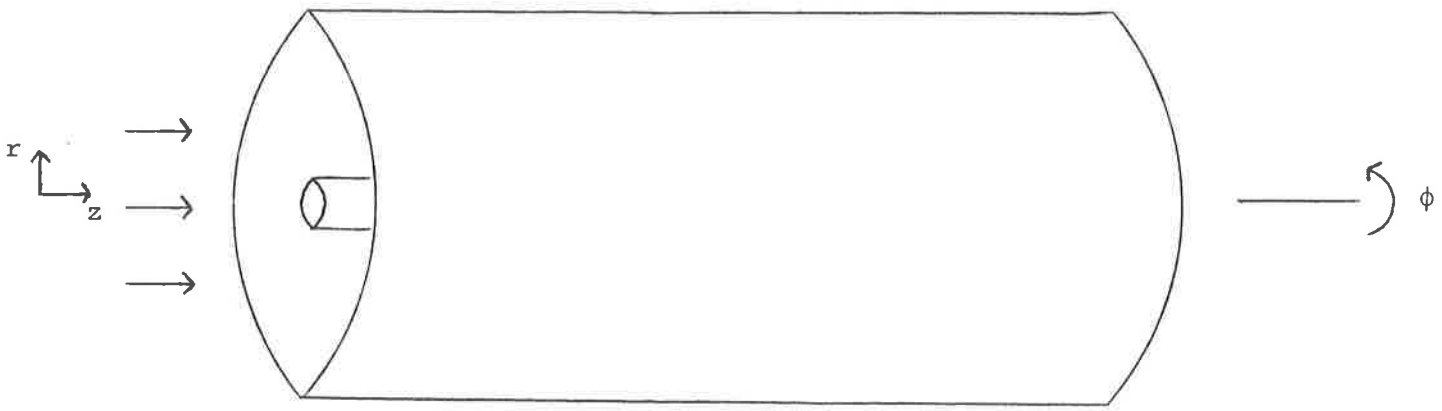

Figure 2

The tunnel is 3 units long and 2 units in diameter. The solid cylindrical step, whose axis lies along that of the tunnel, has a diameter of 0.4 units and is located 0.6 units along the tunnel. At the left an inflow boundary condition is applied, and at the right, where the exit velocity is always supersonic, all gradients are assumed to vanish. We assume axial symmetry, i.e. we consider the flow in a plane ϕ = constant, where ϕ is the angle in cylindrical polar coordinates, (see Figure 2). This problem is similar to the wind tunnel

problem of Emery [7], and also to that of Woodward and Colella [8], in the case of slab symmetry.

The equations of motion governing the flow are the 'two-dimensional' Euler equations in cylindrical polar coordinates with axial symmetry, namely equations (4.1)-(4.2). We assume that the incoming gas is ideal with $\gamma = 1.4$. The initial conditions in the tunnel are given by

$$\left.\begin{aligned} \rho(R,z,0) &= \rho_0 = 1.4 \\ u(R,z,0) &= u_0 = 0 \\ v(R,z,0) &= v_0 = 3 \\ p(R,z,0) &= p_0 = 1 \end{aligned}\right\} \quad \text{all } r,z \ .$$

Gas is continually fed in at the left hand boundary with the flow variables given by $(\rho,u,v,p) = (\rho_0,u_0,v_0,p_0)$, (see Figure 3).

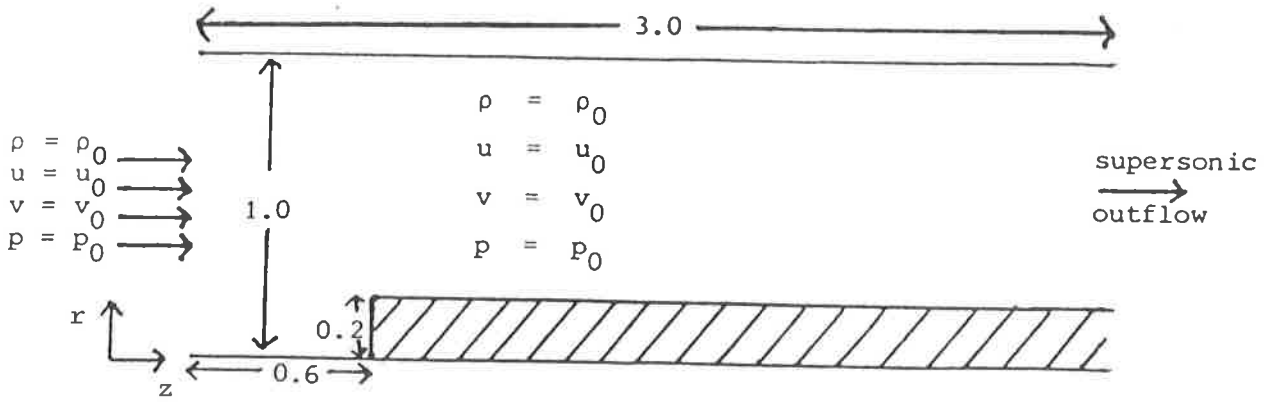

Figure 3

(N.B. Recall that the velocity components in the R,z directions are u,v, respectively.) Along the walls of the tunnel we apply

reflecting boundary conditions. Specifically, along a boundary given by z = constant, we consider an image cell and impose equal density, pressure and tangential velocity, and equal and opposite normal velocity at either end of the cell, i.e. ρ, p, u, v respectively, in this case. A similar argument applies for a reflecting boundary condition given by R = constant.

The main features of the solution are the Mach reflection of a bow shock at the upper wall, making the density distribution the most difficult of the three components to compute, and a rarefaction fan centred at the corner of the step.

Figures 4a-7d are with 120 mesh points in the z-direction and 40 mesh points in the R-direction, i.e. $\Delta R = \Delta z = \frac{1}{40}$. All computations have been done using a second order entropy satisfying scheme with the 'superbee' limiter, (see [6]). The results for the density are output at times $t = j/8$, $j = 1,2,\ldots,16$ using a time step $\Delta t = 0.0025$ so that the maximum C.F.L. number is 0.4. In each case 31 equally spaced contours have been drawn, i.e. at $\rho_{min} + \frac{i}{30}(\rho_{max} - \rho_{min})$, $i = 0,1,\ldots,30$, where ρ_{min}, ρ_{max} are the minimum and maximum densities throughout the flow, respectively.

The c.p.u. time used to compute these results using an Amdahl V7 is as follows:-

Using 'superbee' with the modified entropy satisfying scheme and 120 × 40 mesh points takes 2.0 c.p.u. seconds to compute one time step and a total of 50 c.p.u. seconds to reach a real time of 0.125 seconds using 25 time steps.

(N.B. (a) These figures are for a maximum C.F.L. of 0.8.

(b) For a 60 × 20 mesh the total c.p.u. time taken will be approximately $\frac{1}{8}$ of the values quoted above, e.g. a total of 6.25 c.p.u. seconds would be required to reach a real time of 0.125 seconds.)

Results for the corresponding problem in slab symmetry have been given by Glaister [9] using the approximate Riemann solver of Roe [1]. A comparison of the corresponding times in [9] and those obtained here shows that there is a $33\frac{1}{3}\%$ increase in c.p.u. time due to the different geometry.

Problem 2

This two-dimensional shock tube problem can be considered either in (x,y) or (R,z) geometry, (see Glaister [10]).

Consider the two-dimensional Euler equations with slab symmetry or axial symmetry and the region $(x,y) \in [0,1] \times [0,1]$ or $(R,z) \in [0,1] \times [0,1]$ with rigid boundaries along $x = 0$, $y = 0$ or $R = 0$, $z = 0$. We position a membrane along (x,y) or (R,z) where $\sqrt{x^2 + y^2} = \frac{1}{2}$ or $\sqrt{R^2 + z^2} = \frac{1}{2}$ and have initial data

$$(\rho,u,v,p) = \begin{cases} (\rho_L,0,0,p_L) & \sqrt{x^2 + y^2} < \frac{1}{2} \text{ or } \sqrt{R^2 + z^2} < \frac{1}{2} \\ (\rho_R,0,0,p_R) & \sqrt{x^2 + y^2} > \frac{1}{2} \text{ or } \sqrt{R^2 + z^2} > \frac{1}{2} \end{cases}.$$

The solution to this problem has cylindrical or spherical symmetry and satisfies the corresponding 'one-dimensional' Euler equations (see Glaister [10]). Thus we can see whether the solution remains symmetric: moreover, we can compare the results with those obtained using a 'one-

dimensional' algorithm for the Euler equations with cylindrical or spherical symmetry.

Figures 8-11 refer to the cylindrical problem and the two-dimensional results have been computed using the algorithm of §3 in (x,y) cartesian geometry, i.e. using the approximate Riemann solver of Roe [1]. Figures 12-15 refer to the spherical problem and the two-dimensional results have been computed using the algorithm of §4 in (R,z) cylindrical geometry. In each case we take $\gamma = 1.4$, a mesh with 50×50 grid points and a time step $\Delta t = 0.004$. For each output time we draw 31 equally spaced contours at $\rho_{min} + \frac{i}{30} (\rho_{max} - \rho_{min})$, $i = 0,1,\ldots,30$, where ρ_{min}, ρ_{max} are the minimum and maximum densities throughout the flow, respectively. In addition we plot the density along $x = y$ or $R = z$ and plot the solution to the corresponding one-dimensional cylindrical or spherical problem obtained using the algorithm of Glaister [2] with 50 and 800 points. The one-dimensional solution with 800 points provides a good approximation to the exact solution, whereas the solution with 50 points provides a comparison on similar grids.

The initial discontinuity breaks up into a converging shock and contact discontinuity. The shock is reflected from $x = y = 0$ or $R = z = 0$ and interacts with the contact discontinuity. This results in a transmitted shock together with the contact discontinuity still converging. These features are apparent in Figures 8 or 12, 9 or 13, 10 or 14, 11 or 15, respectively. For each figure we see that the two-dimensional solution obtained remains symmetrical and is comparable to the one-dimensional solution on a similar grid. Furthermore, the solution clearly models the high resolution solution obtained with 800 points.

The c.p.u. time used to compute these results using an Amdahl V7 is as follows.

Using 'superbee' with the modified entropy satisfying scheme and 50 × 50 mesh points takes;-

(a) Cylindrical case.

1.05 c.p.u. seconds to compute one time step and

52.5 c.p.u. seconds to reach a real time of

0.2 seconds using 50 time steps

(b) spherical case.

1.2 c.p.u. seconds to compute one time step and

60.0 c.p.u.seconds to reach a real time of

0.2 seconds using 50 time steps.

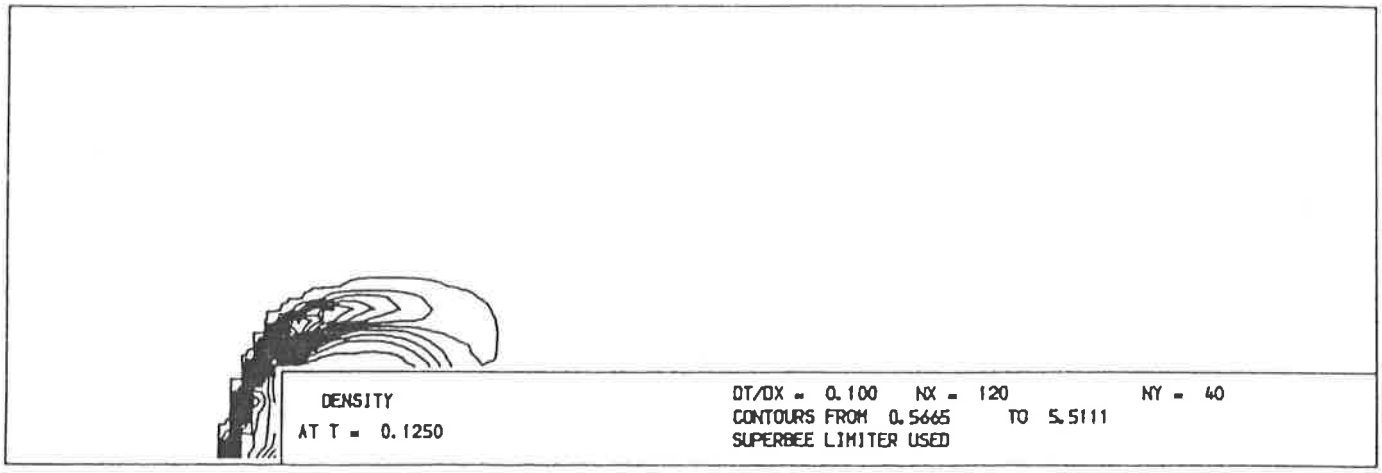

Figure 4a

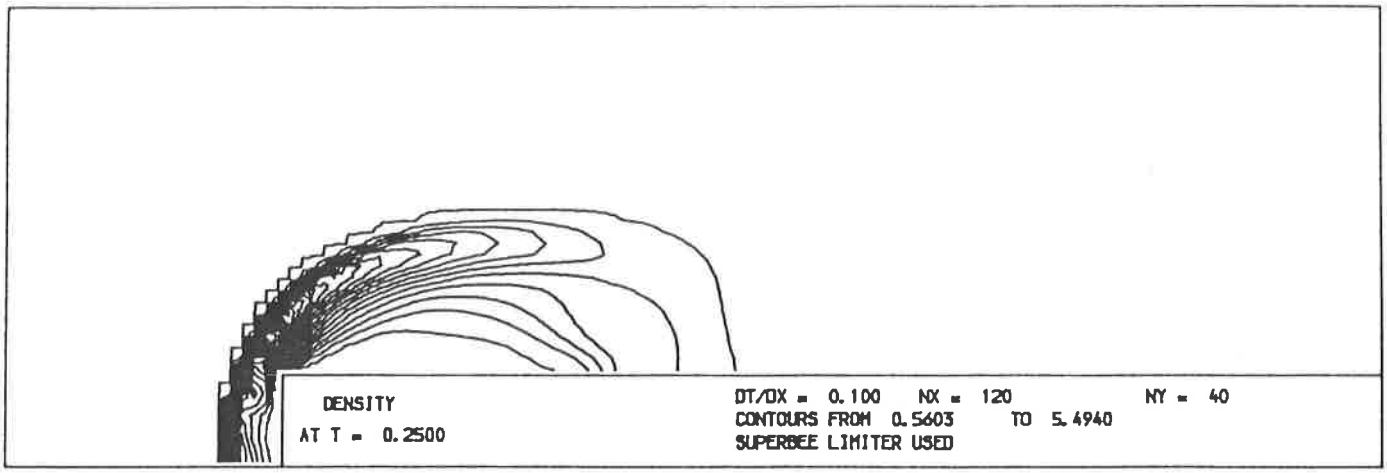

Figure 4b

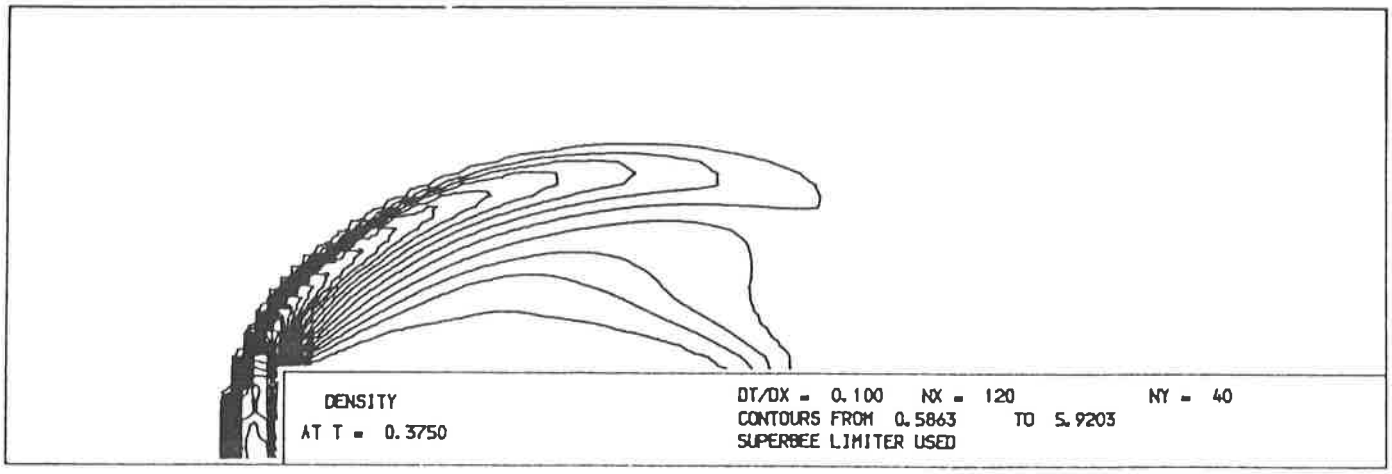

Figure 4c

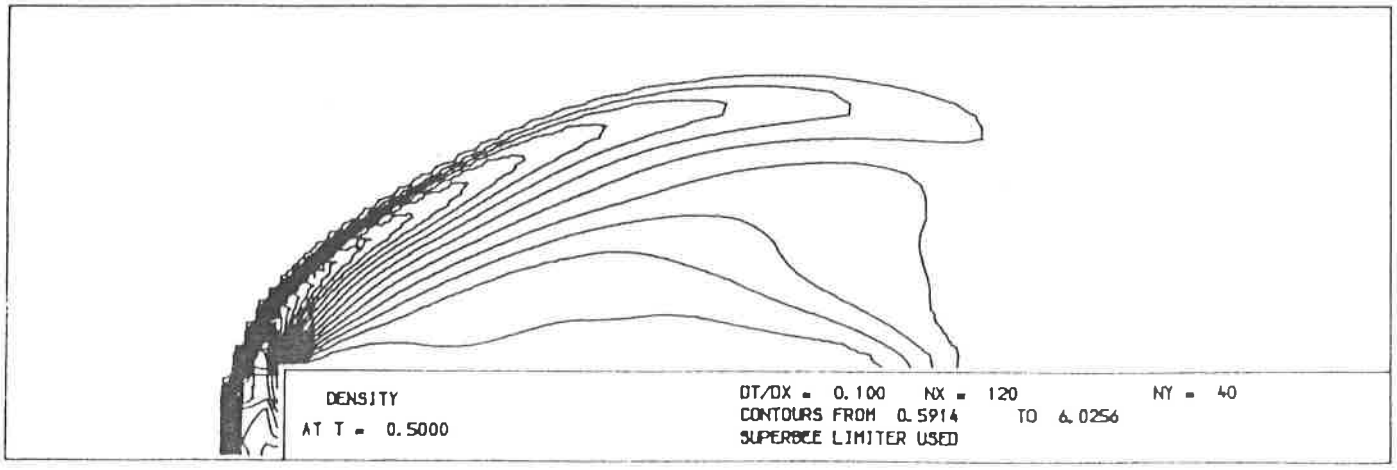

Figure 4d

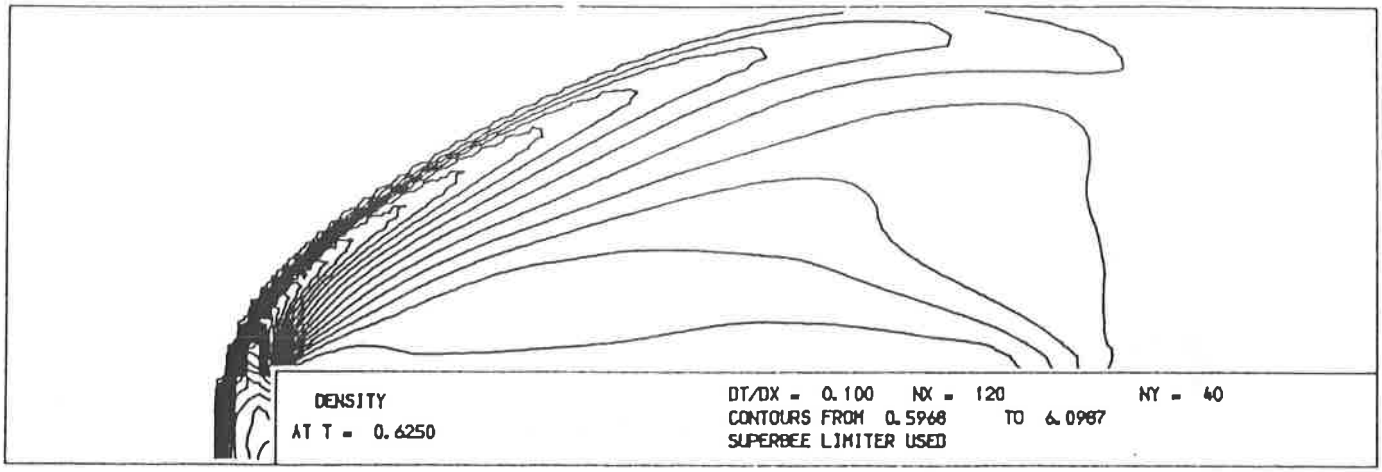

Figure 5a

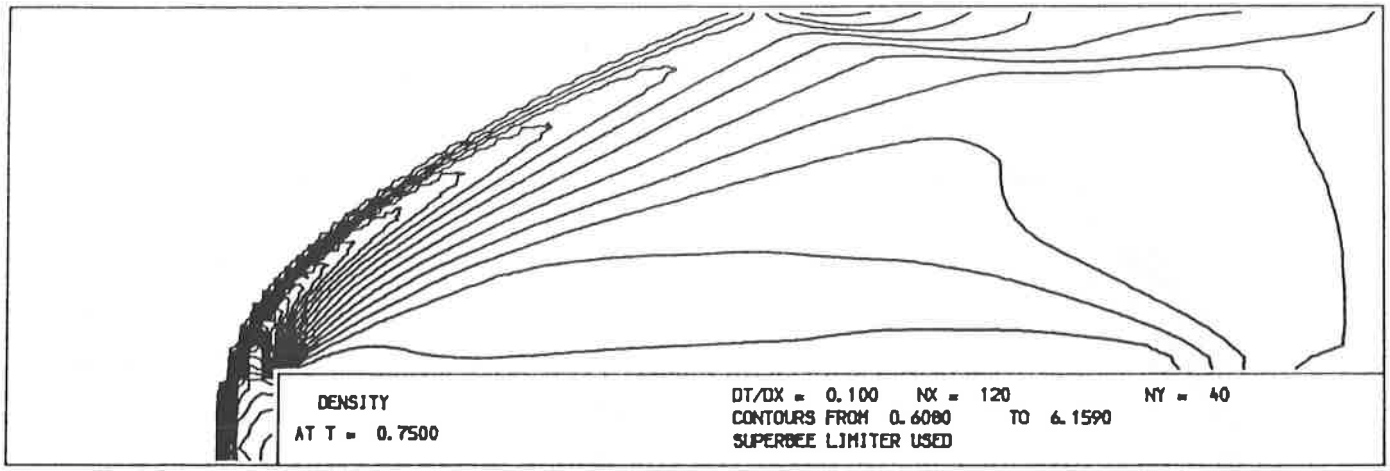

Figure 5b

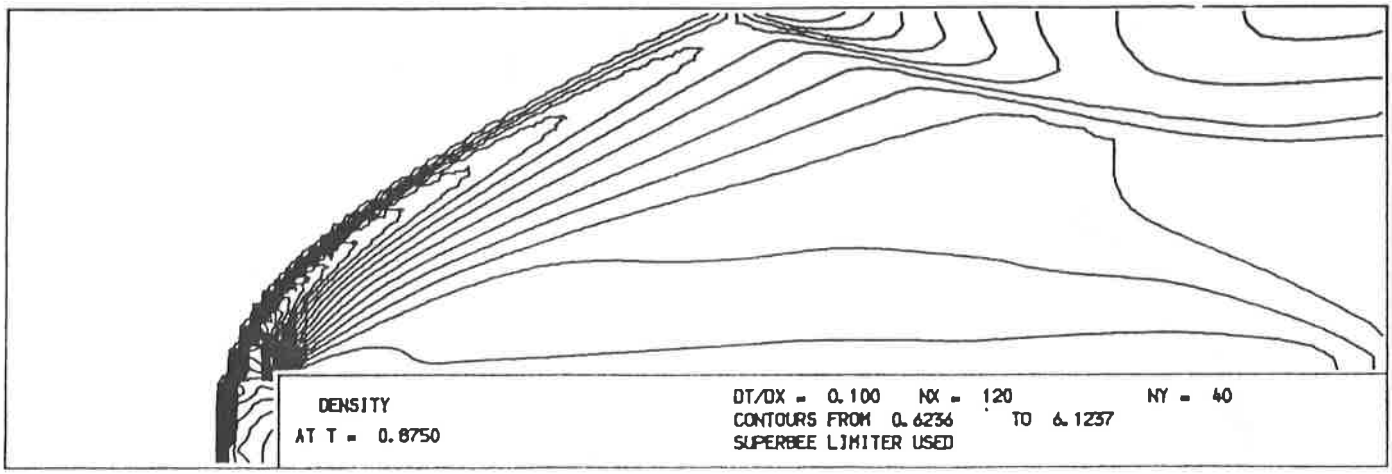

Figure 5c

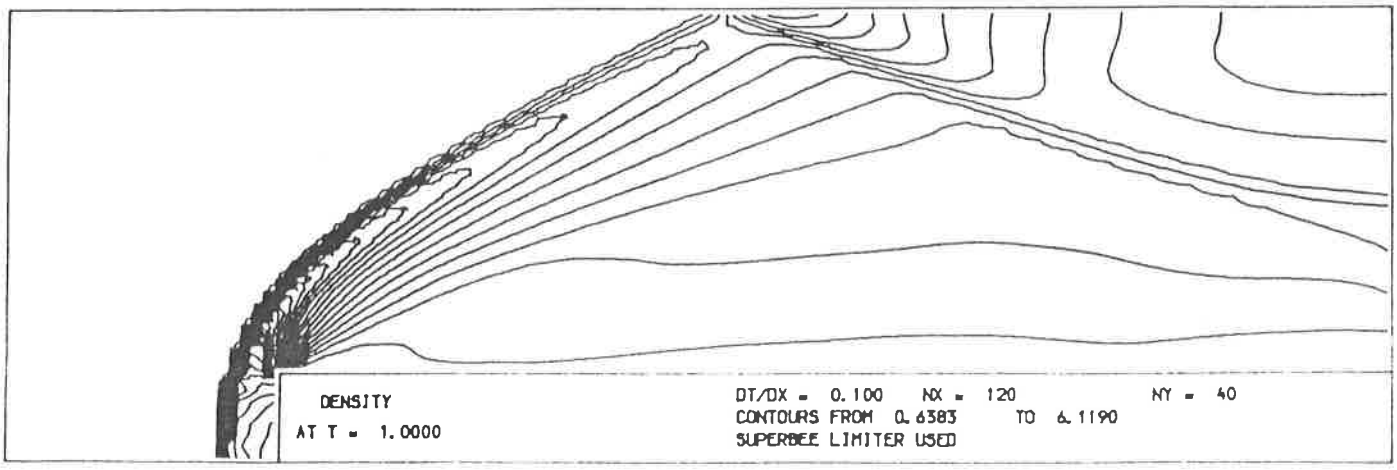

Figure 5d

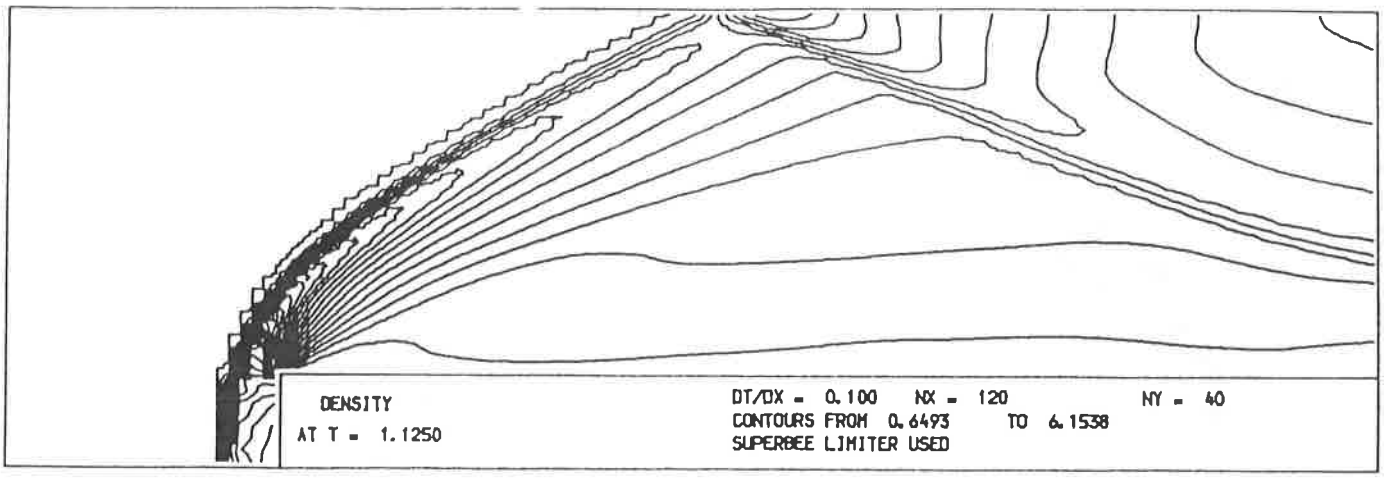

Figure 6a

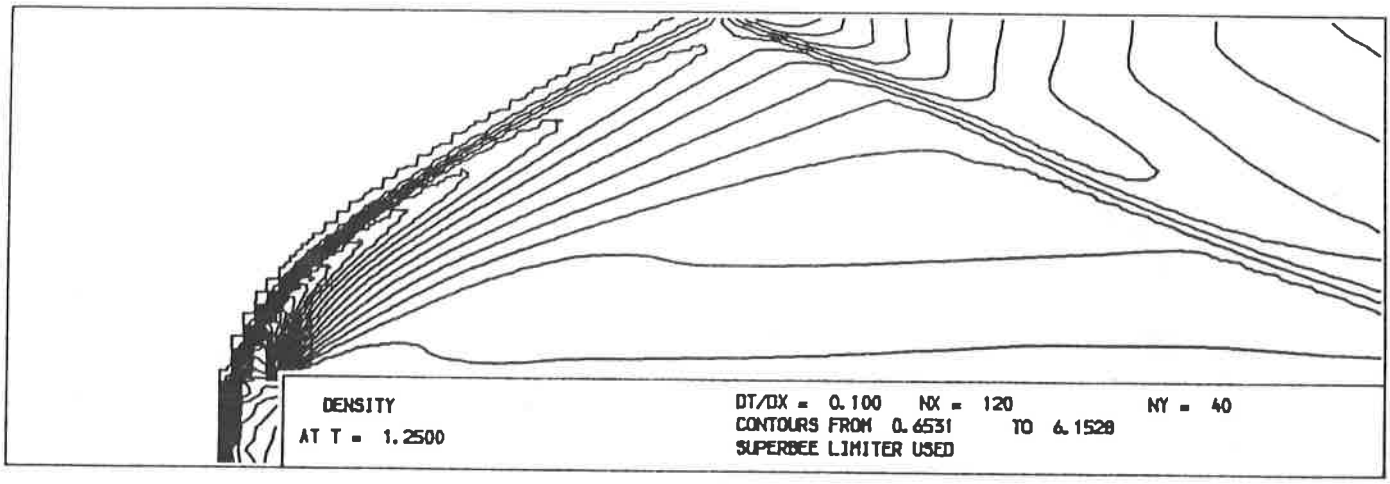

Figure 6b

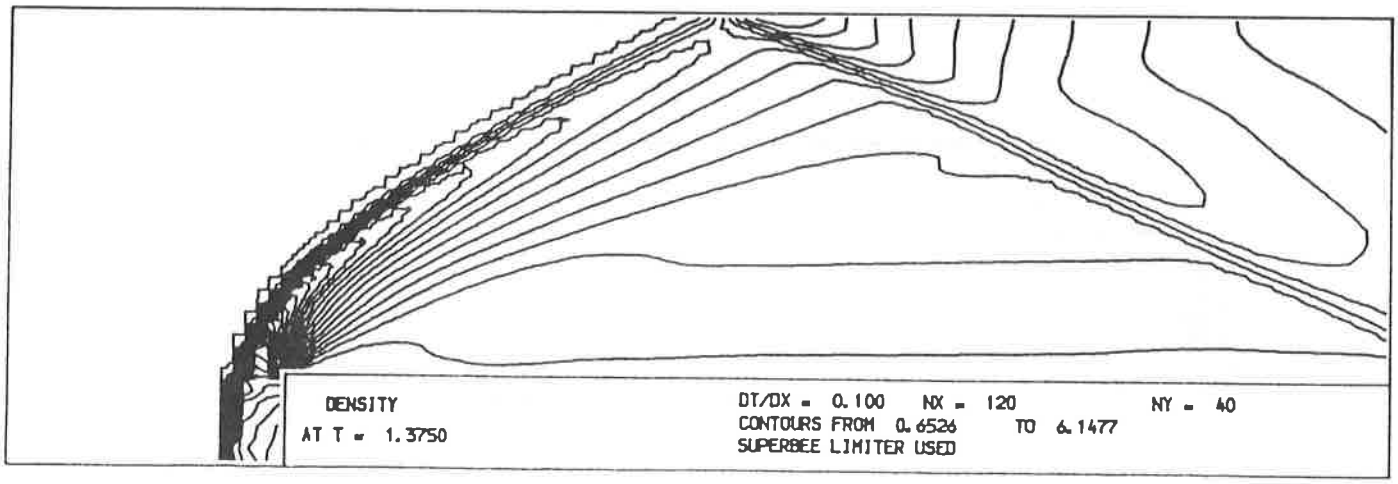

Figure 6c

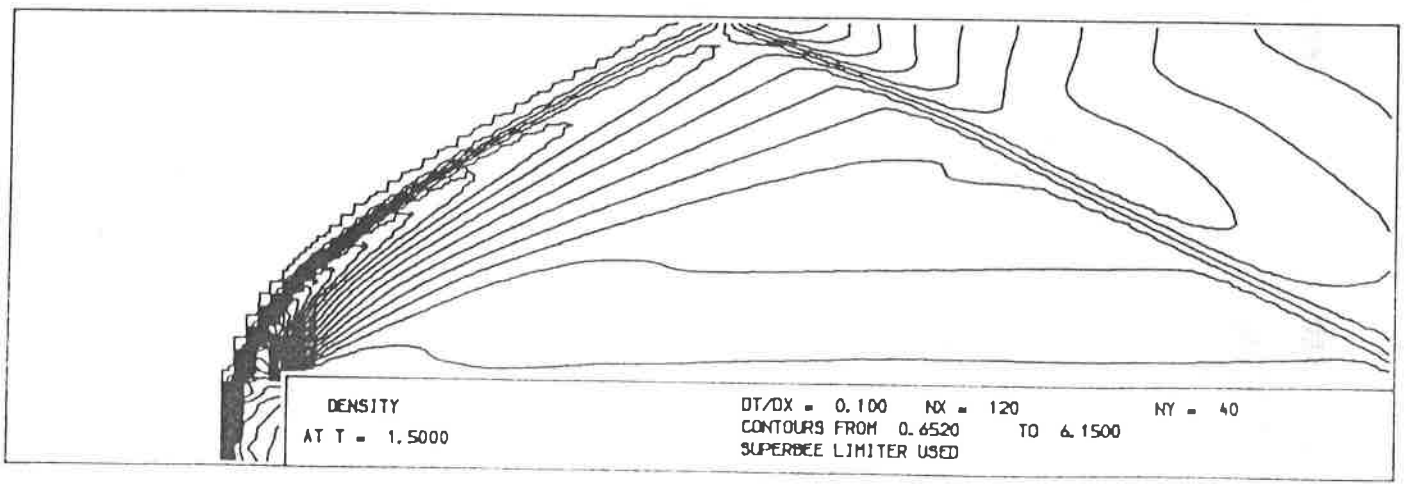

Figure 6d

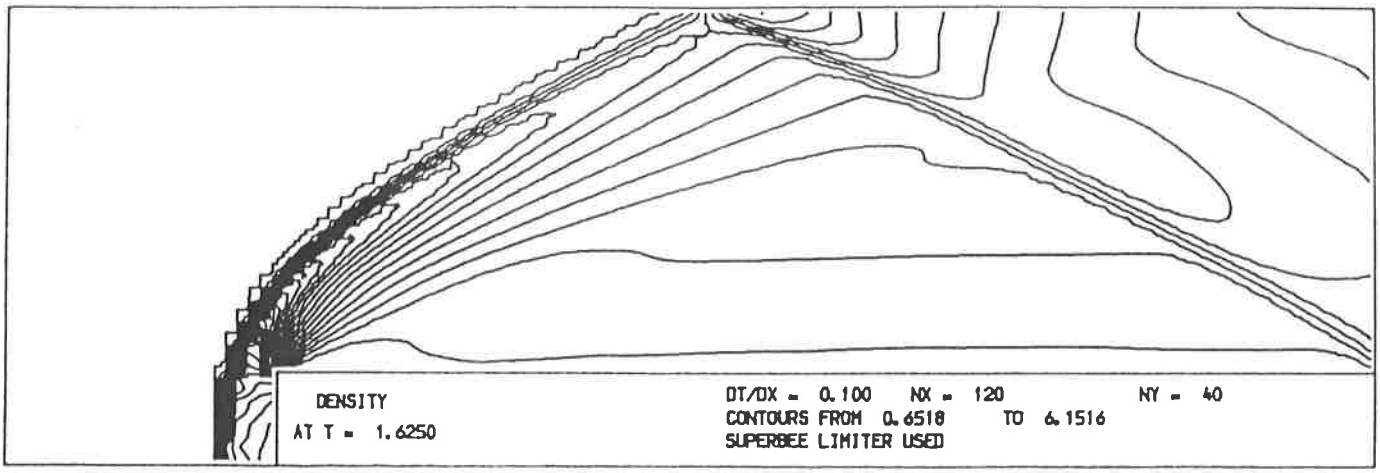

Figure 7a

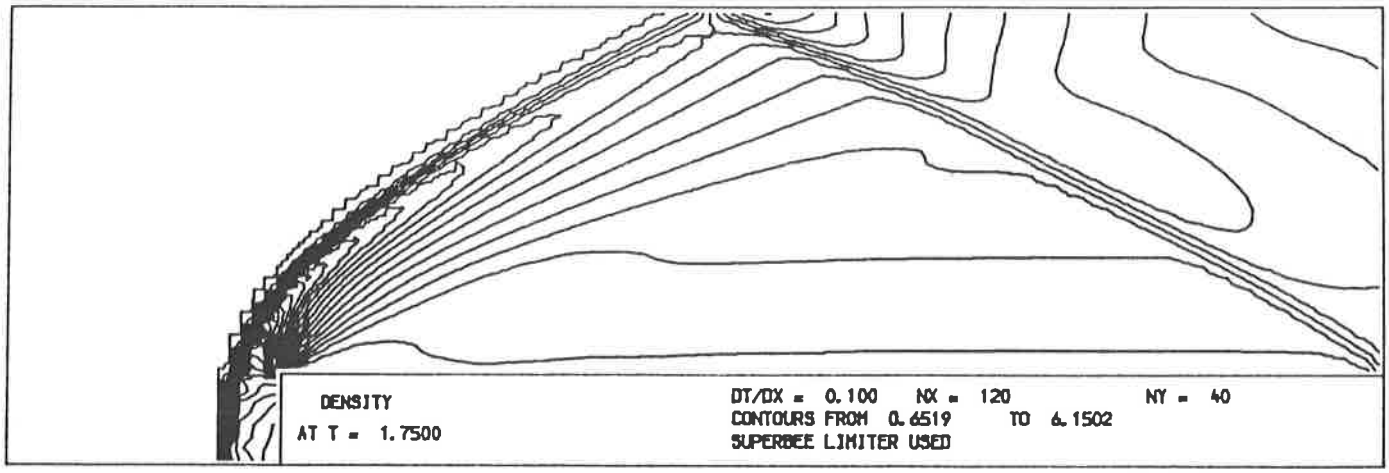

Figure 7b

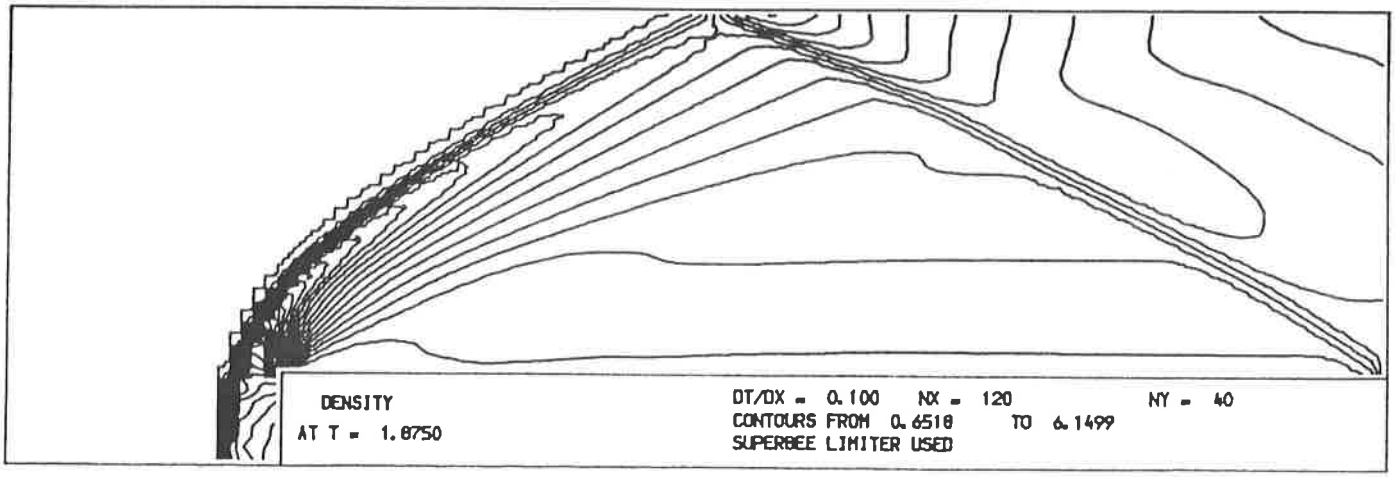

Figure 7c

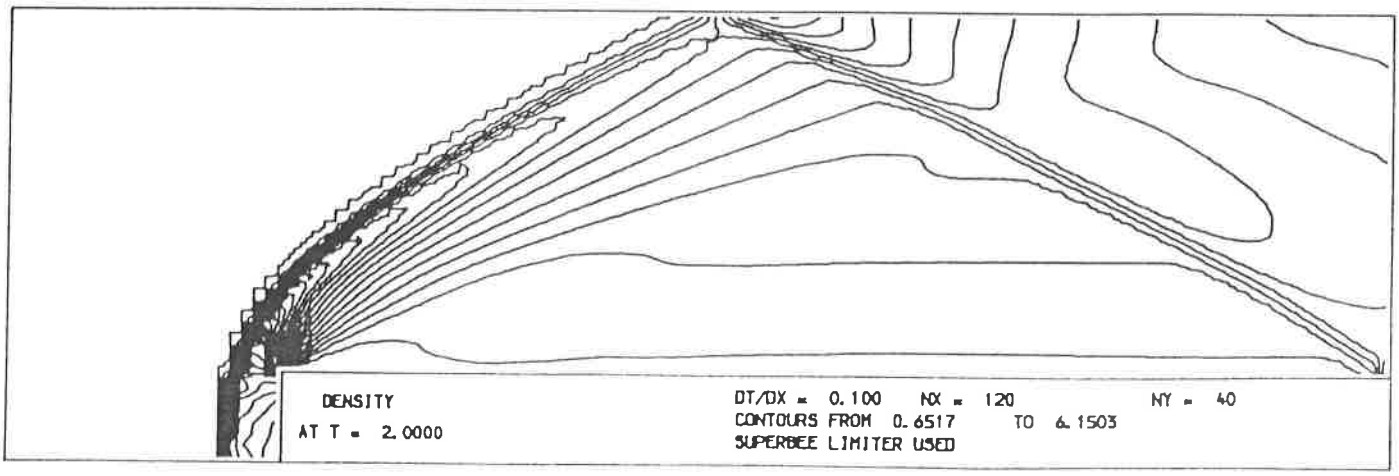

Figure 7d

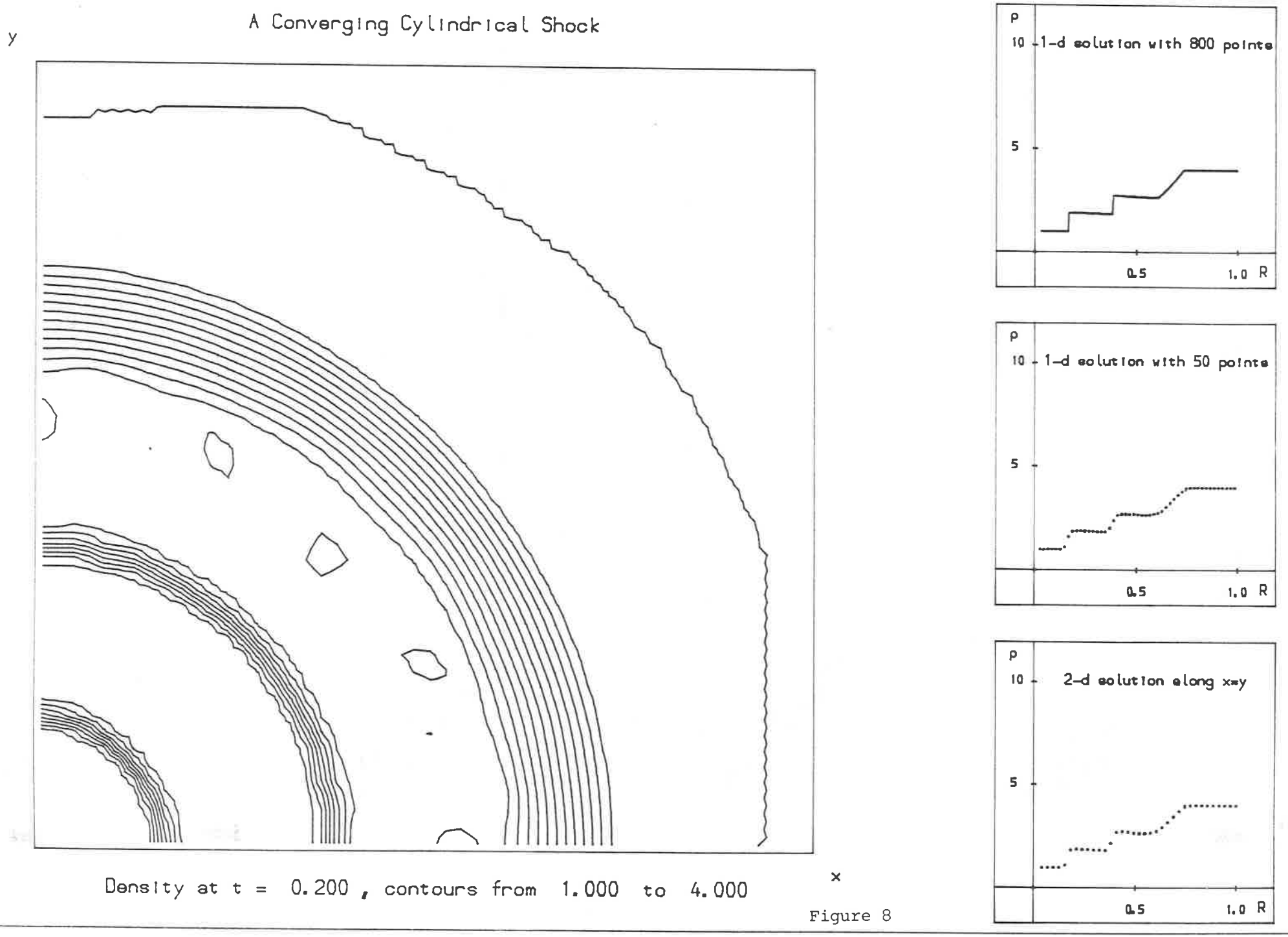
A Converging Cylindrical Shock
y
x
Density at t = 0.200 , contours from 1.000 to 4.000
ρ
10
1-d solution with 800 points
5
0.5
1.0 R
ρ
10
1-d solution with 50 points
5
0.5
1.0 R
ρ
10
2-d solution along x=y
5
0.5
1.0 R

Figure 8

A Converging Cylindrical Shock

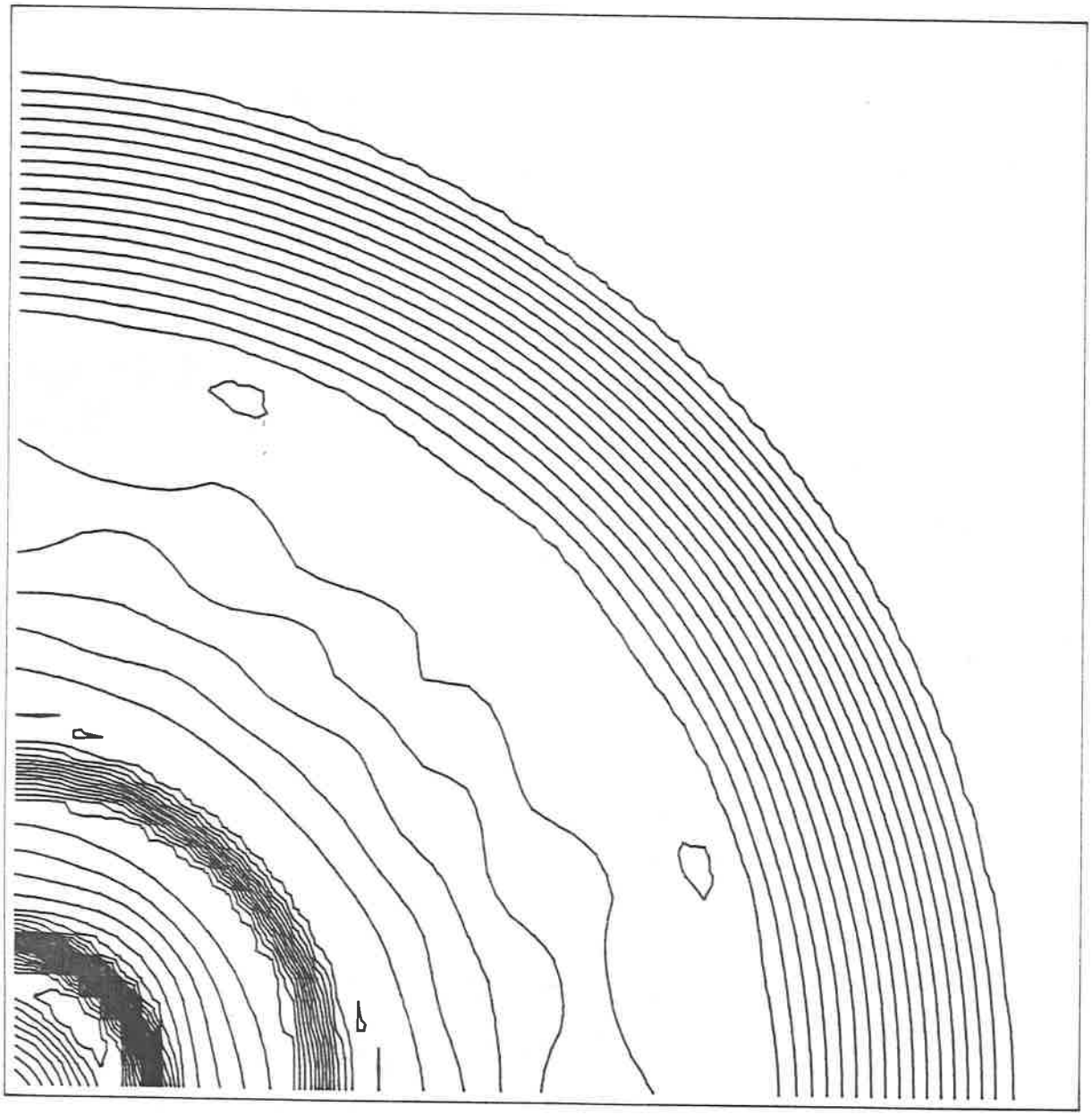

Density at t = 0.360 , contours from 2.301 to 4.226

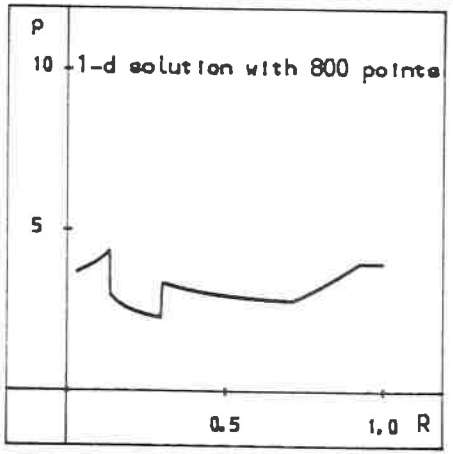

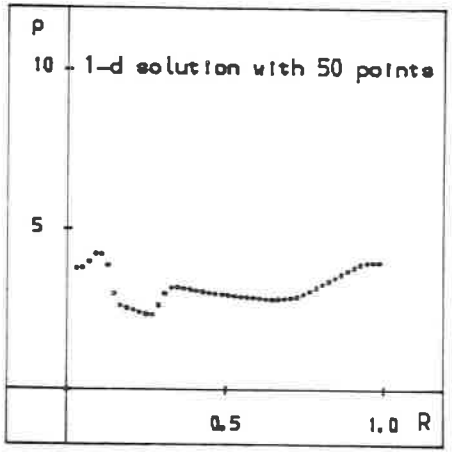

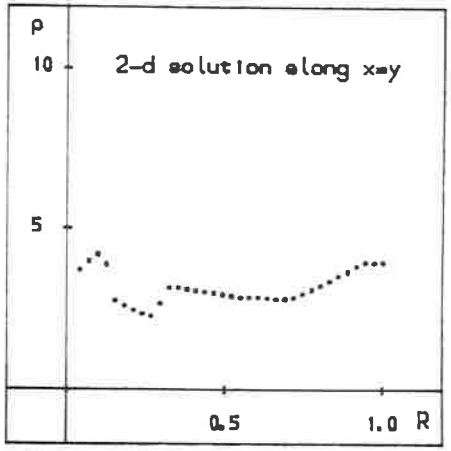

Figure 9

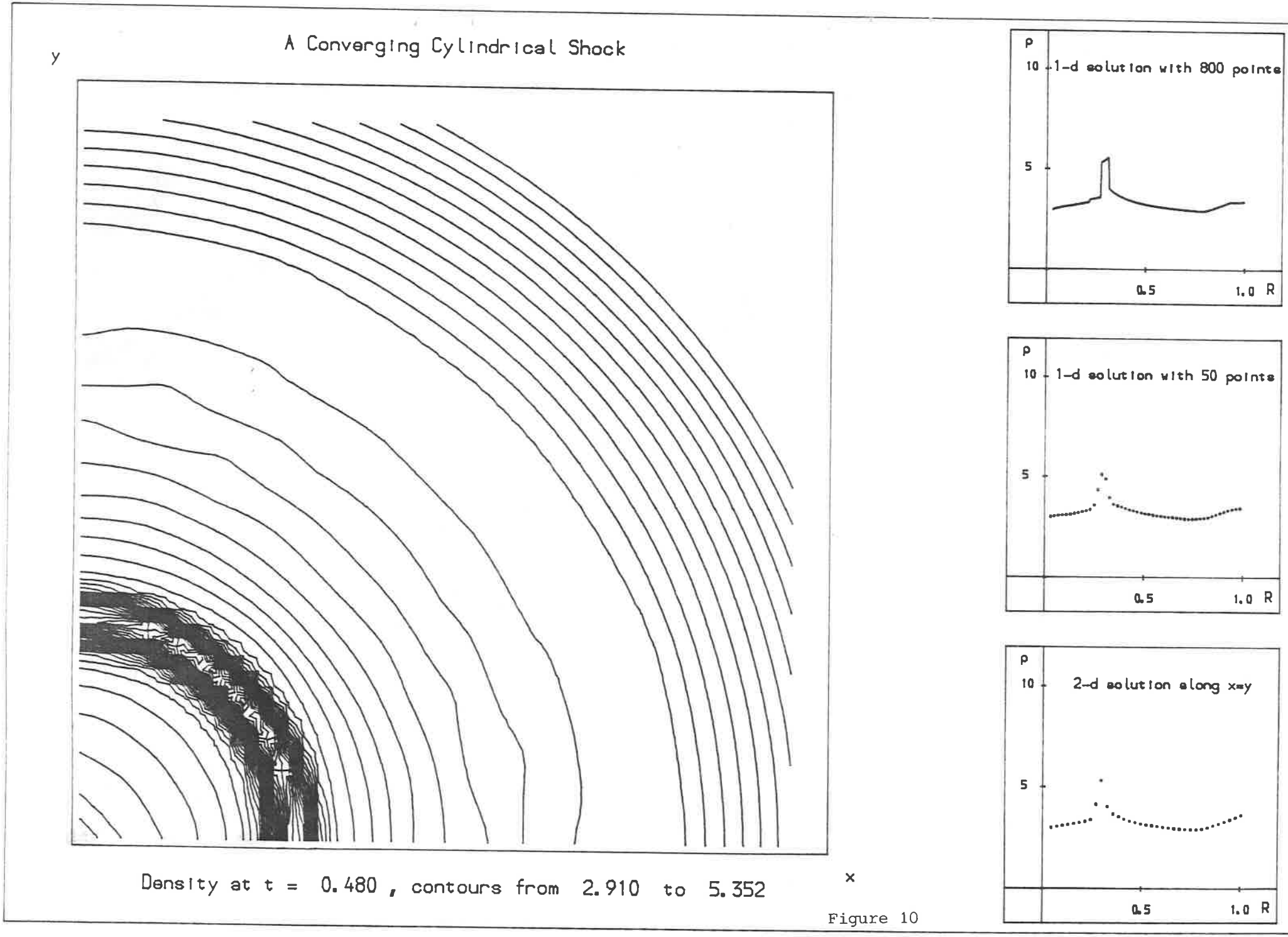
A Converging Cylindrical Shock
y
x
Density at t = 0.480 , contours from 2.910 to 5.352
ρ
10
1-d solution with 800 points
5
0.5
1.0 R
ρ
10
1-d solution with 50 points
5
0.5
1.0 R
ρ
10
2-d solution along x=y
5
0.5
1.0 R

Figure 10

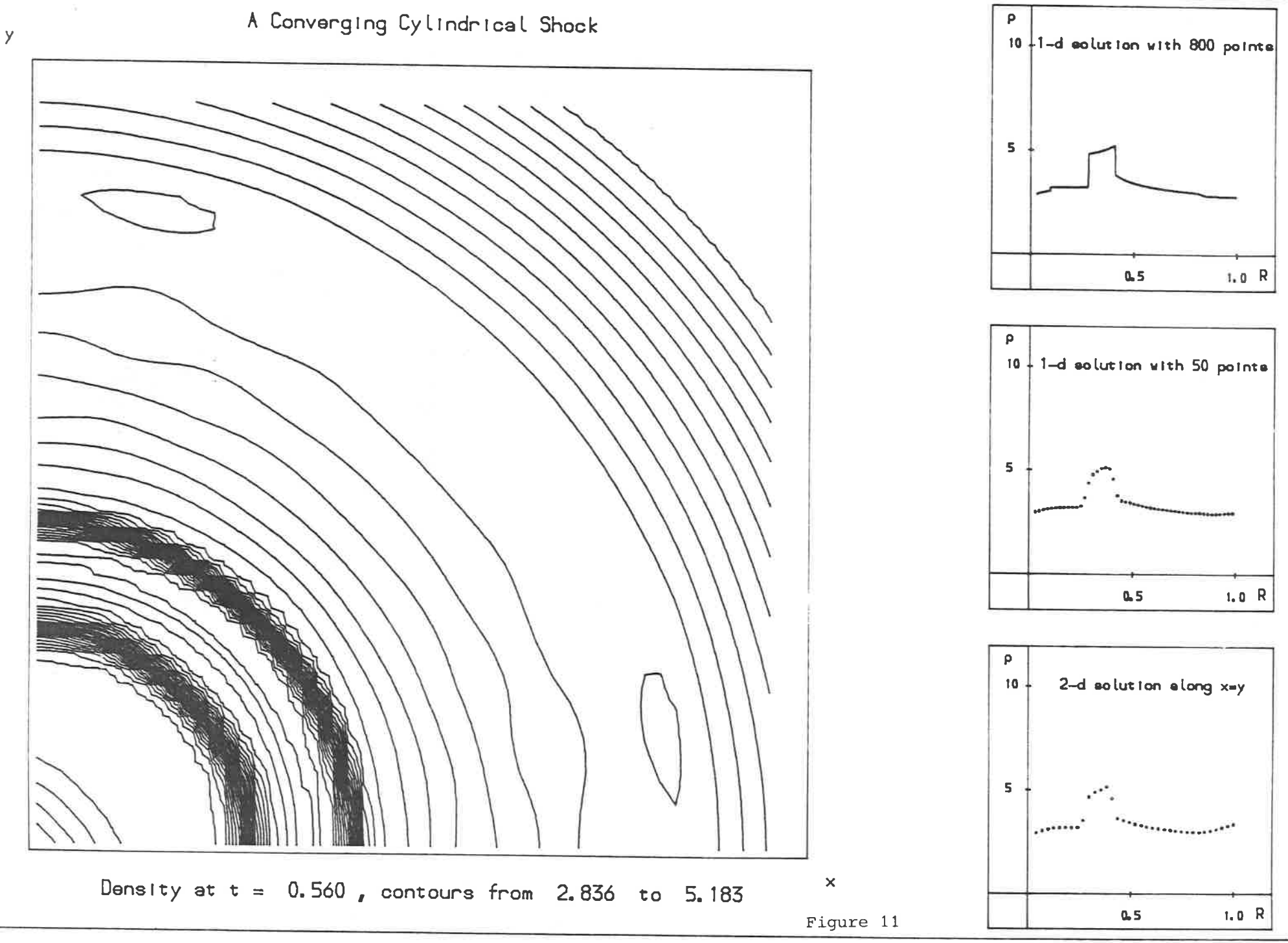
A Converging Cylindrical Shock
y
x
Density at t = 0.560 , contours from 2.836 to 5.183
ρ
10
5
1-d solution with 800 points
0.5
1.0 R
ρ
10
5
1-d solution with 50 points
0.5
1.0 R
ρ
10
5
2-d solution along x=y
0.5
1.0 R

Figure 11

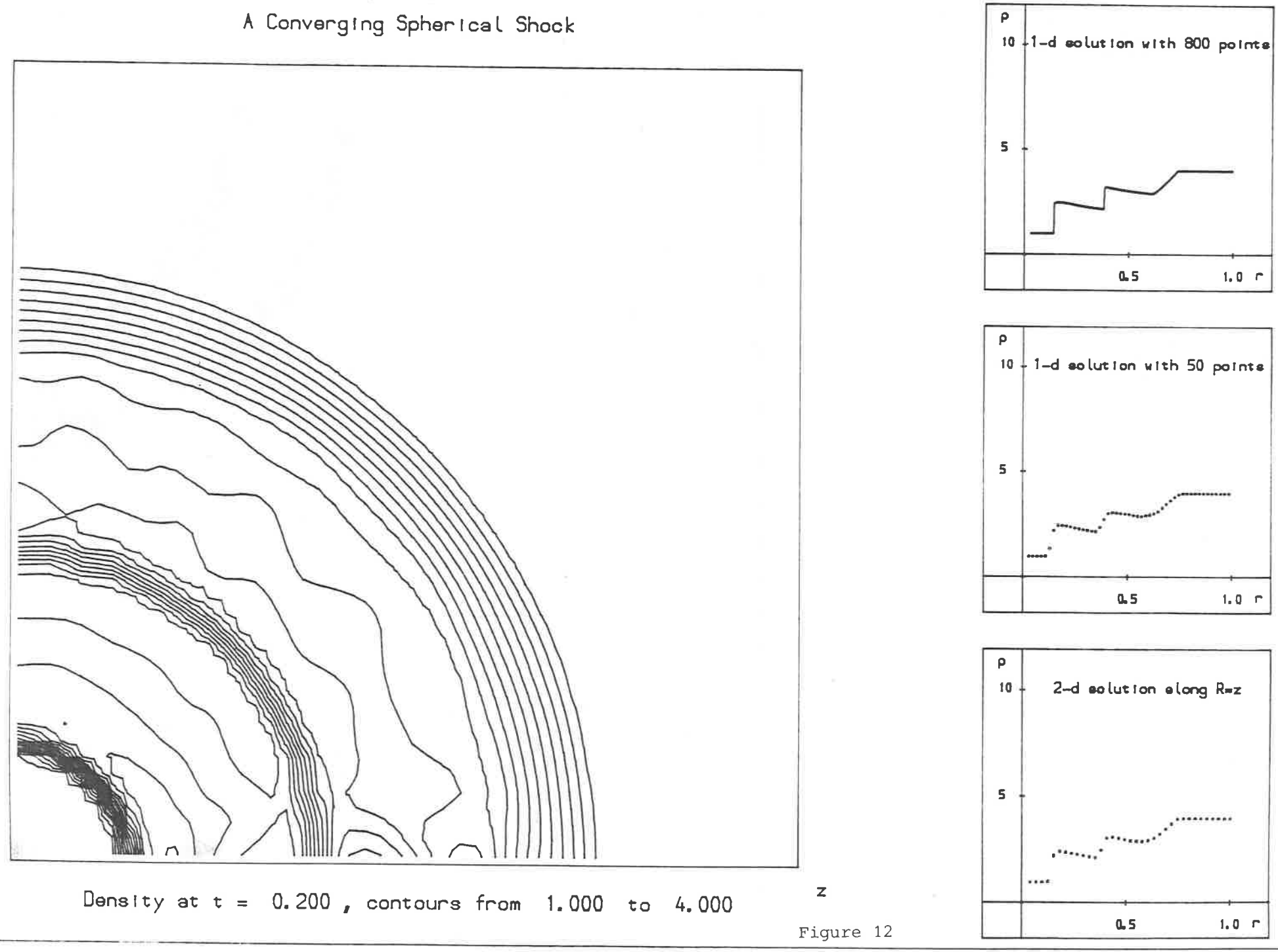
A Converging Spherical Shock
R
z
Density at t = 0.200 , contours from 1.000 to 4.000
ρ
10
5
1-d solution with 800 points
0.5
1.0 r
ρ
10
5
1-d solution with 50 points
0.5
1.0 r
ρ
10
5
2-d solution along R=z
0.5
1.0 r

Figure 12

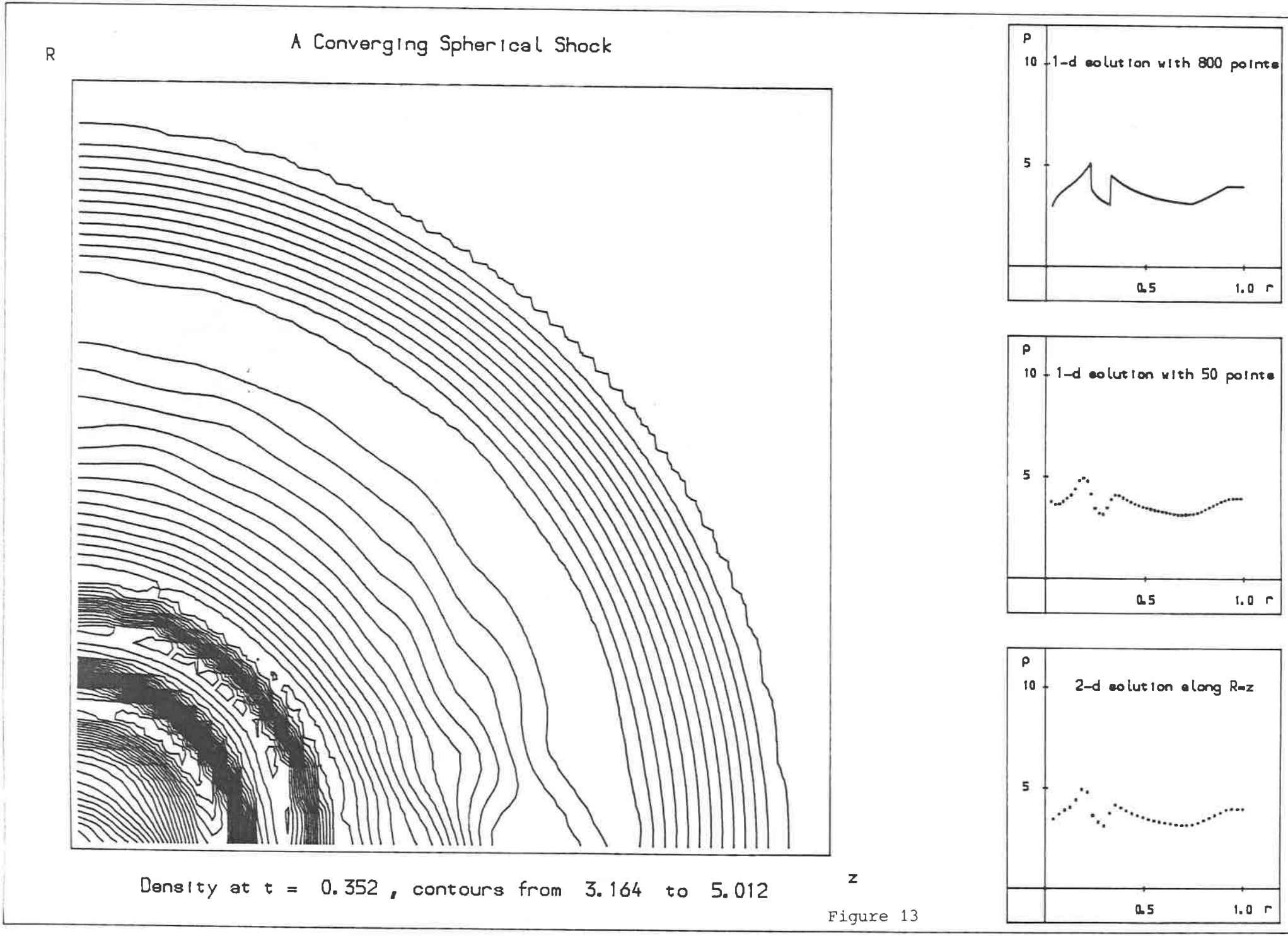
A Converging Spherical Shock
R
Density at t = 0.352 , contours from 3.164 to 5.012
z
ρ
10
1-d solution with 800 points
5
0.5
1.0 r
ρ
10
1-d solution with 50 points
5
0.5
1.0 r
ρ
10
2-d solution along R=z
5
0.5
1.0 r

Figure 13

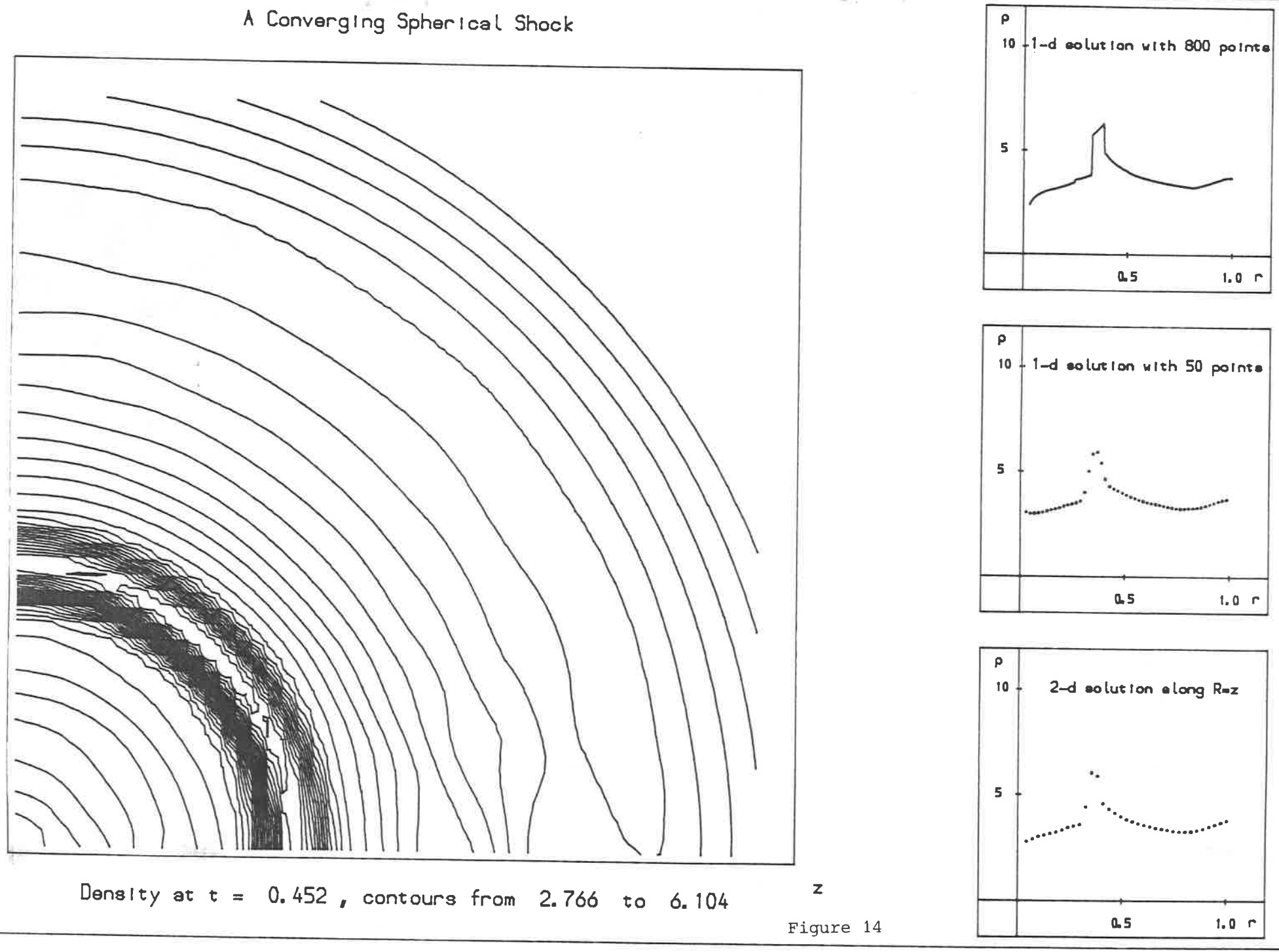
A Converging Spherical Shock
R
z
Density at t = 0.452 , contours from 2.766 to 6.104
ρ
10
5
1-d solution with 800 points
0.5
1.0 r
ρ
10
5
1-d solution with 50 points
0.5
1.0 r
ρ
10
5
2-d solution along R=z
0.5
1.0 r

Figure 14

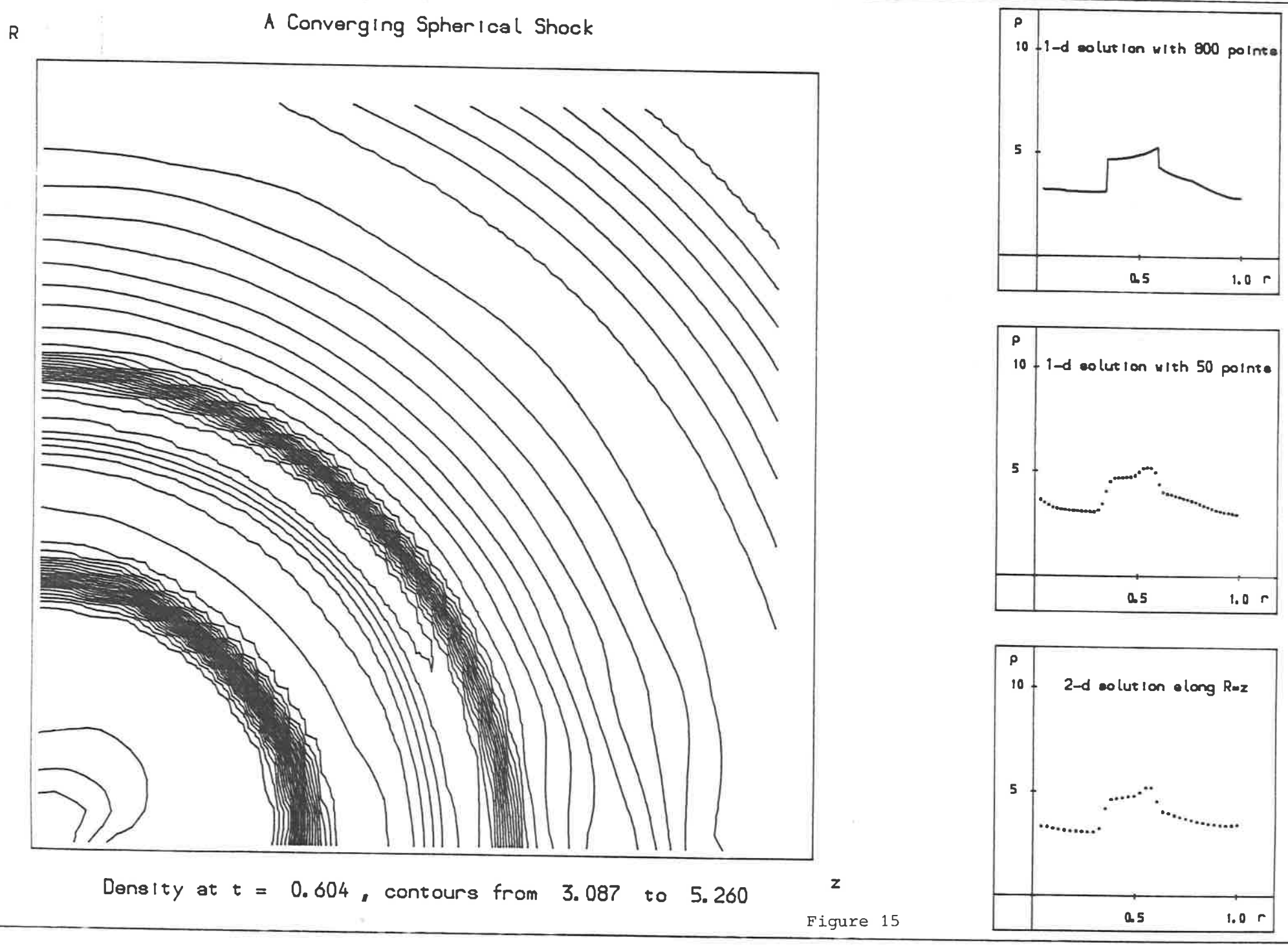
A Converging Spherical Shock
R
z
Density at t = 0.604 , contours from 3.087 to 5.260
ρ
10
5
1-d solution with 800 points
0.5
1.0 r
ρ
10
5
1-d solution with 50 points
0.5
1.0 r
ρ
10
5
2-d solution along R=z
0.5
1.0 r

Figure 15

6. CONCLUSIONS

We have proposed an algorithm for the Euler equations in a general orthogonal curvilinear coordinate system. This algorithm, which is an extension of the schemes of Roe [1] and Glaister [2], incorporates the technique of operator splitting. The algorithm has been applied to two test problems with axial symmetry and has achieved satisfactory results.

ACKNOWLEDGEMENTS

I would like to express my thanks to Dr. M. J. Baines for useful discussions.

I acknowledge the financial support of A.W.R.E. Aldermaston.

REFERENCES

1. P.L. ROE, Approximate Riemann Solvers, Parameter Vectors and Difference Schemes, J. Comput. Phys. 43, 357(1981).

2. P. GLAISTER, Flux Difference Splitting Techniques for the Euler Equations in Non-Cartesian Geometry. Numerical Analysis Report 8-85, University of Reading, 1985.

3. P.L. ROE, Upwind Differencing Schemes, Hyperbolic Conservation Laws with Source Terms, 1st Int. Congress on Hyperbolic Problems, St. Etienne, (ed. C. Carassa, D. Serre), (to appear), 1986.

4. P.L. ROE, Some Contributions to the Modelling of Discontinuous Flows, Proc. AMS/SIAM Seminar, San Diego, (1983).

5. P.L. ROE and J. PIKE, Efficient Construction and Utilisation of Approximate Riemann Solutions, Computing Methods in Applied Science and Engineering VI, 499 (1984).

6. P.K. SWEBY, High Resolution Schemes using Flux Limiters for Hyperbolic Conservation Laws, SIAM J. Numer. Anal. 21, 995 (1984).

7. A.F. EMERY, An Evaluation of Several Differencing Methods for Inviscid Fluid Flow Problems, J. Comput. Phys., 2, 306 (1968).

8. P. WOODWARD and P. COLELLA, The Numerical Simulation of Two-Dimensional Fluid Flow with strong shocks. J. Comput. Phys., 54, 115 (1984).

9. P. GLAISTER, An Approximate Linearised Riemann Solver for the Three Dimensional Euler Equations with a General Equation of State, Numerical Analysis Report 11-86, University of Reading, 1986.

10. P. GLAISTER, Similarity Solutions for Shock Reflection Problems in Gas Dynamics, Numerical Analysis Report 13-86, University of Reading, 1986.